



HAL
open science

Co-encapsulation of flavonoids with anti-cancer drugs : A challenge ahead

Morgane Renault-Mahieux, Nathalie Mignet, Johanne Seguin, Khair
Alhareth, Muriel Paul, Karine Andrieux

► To cite this version:

Morgane Renault-Mahieux, Nathalie Mignet, Johanne Seguin, Khair Alhareth, Muriel Paul, et al..
Co-encapsulation of flavonoids with anti-cancer drugs: A challenge ahead. *International Journal of
Pharmaceutics*, 2022, 623, pp.121942. 10.1016/j.ijpharm.2022.121942 . hal-03882629

HAL Id: hal-03882629

<https://hal.science/hal-03882629v1>

Submitted on 22 Jul 2024

HAL is a multi-disciplinary open access archive for the deposit and dissemination of scientific research documents, whether they are published or not. The documents may come from teaching and research institutions in France or abroad, or from public or private research centers.

L'archive ouverte pluridisciplinaire **HAL**, est destinée au dépôt et à la diffusion de documents scientifiques de niveau recherche, publiés ou non, émanant des établissements d'enseignement et de recherche français ou étrangers, des laboratoires publics ou privés.



Distributed under a Creative Commons Attribution - NonCommercial - NoDerivatives 4.0
International License

1 Co-encapsulation of flavonoids with anti-cancer 2 drugs: a challenge ahead

3 Morgane Renault-Mahieux^{1,2}, Nathalie Mignet¹, Johanne Seguin¹, Khair Alhareth¹, Muriel
4 Paul², Karine Andrieux^{1*}

5 1. Université Paris Cité, CNRS, Inserm, UTCBS, F-75006 Paris, France ; nathalie.mignet@u-
6 paris.fr; johanne.seguin@u-paris.fr; khairallah.alhareth@u-paris.fr; karine.andrieux@u-
7 paris.fr

8 2. Pharmacy Department, AP-HP, Henri Mondor Hospital Group, F-94010, France ;
9 morgane.renault@aphp.fr; muriel.paul@aphp.fr

10 *. Corresponding author

11

12 Abstract:

13 Flavonoids have been considered as promising molecules for cancer treatment due to their
14 pleiotropic properties such as anti-carcinogenic, anti-angiogenic or efflux proteins inhibition.
15 However, due to their lipophilic properties and their chemical instability, vectorization seems
16 compulsory to administer flavonoids. Flavonoids have been co-encapsulated with other anti-
17 cancer agents in a broad range of nanocarriers aiming to i) achieve a synergistic/additive
18 effect at the tumor site, ii) delay drug resistance apparition by combining agents with different
19 action mechanisms or iii) administer a lower dose of the anti-cancer drug, reducing its
20 toxicity. However, co-encapsulation could lead to a change in the nanoparticles' diameter
21 and drug-loading, as well as a decrease in their stability during storage. The preparation
22 process should also take into accounts the physico-chemical properties of both the flavonoid
23 and the anti-cancer agent. Moreover, the co-encapsulation could affect the release and
24 activity of each drug. This review aims to study the formulation, preparation and
25 characterization strategies of these co-loaded nanomedicines, as well as their stability. The
26 *in vitro* assays to predict the nanomedicines' behavior in biological fluids, as well as their *in*
27 *vivo* efficacy, are also discussed. A special focus concerns the evaluation of their synergistic
28 effect on tumor treatment.

29

30 Keywords: nanomedicine, co-encapsulation, flavonoids, cancer, synergism

31

- 32 Abbreviations:
- 33 ASP: aspirin
- 34 BAI: baicalin
- 35 BCL: baicalein
- 36 CUR: curcumin
- 37 DCK: N^α-deoxycholy-L-lysyl-methylester
- 38 DLS: dynamic light scattering
- 39 DOX: doxorubicin base
- 40 DOX-HCL: doxorubicin hydrochloride
- 41 DTX: docetaxel
- 42 EGCG: (-)-epigallocatechin gallate
- 43 EPR: enhanced permeability and retention
- 44 ETO: etoposide
- 45 GCA: glycyrrhizic acid
- 46 GEN: genistein
- 47 ICA: icaritin
- 48 PMX: pemetrexed
- 49 PLGA: poly(lactic-co-glycolic acid)
- 50 PTX: paclitaxel
- 51 QUE: quercetin
- 52 SEM: scanning electron microscopy
- 53 SGF: simulated gastric fluid
- 54 SIF: simulated intestinal fluid
- 55 SLB: silybin
- 56 TEM: transmission electron microscopy
- 57 TMX: tamoxifen

58 TMZ: temozolomide

59 TPT: topotecan

60 VIN: vincristine sulfate

61

62 1. Introduction

63 Flavonoids exerts interesting anti-cancer effects as well as reversal of anti-cancer drug
64 resistance, or activity towards mechanisms involved in tumor invasion or development. It is
65 common practice to administrate a combination of anti-cancer agents to overcome cross-
66 resistance and achieve synergistically enhanced therapeutic effect, as well as to prevent
67 toxic effects (Bayat Mokhtari et al., 2017). Combining an anti-cancer drug with flavonoids
68 could maximize the treatment efficacy *via* an additional or a synergistic effect, thus allowing
69 the administration of a lower dose of the anti-cancer drug and a decrease in its toxicity. It
70 could also minimize the toxicity of anti-cancer drug treatments by scavenging free radicals,
71 thus counteracting the ROS-mediated damages. Moreover, several flavonoids have been
72 shown to inactivate several drug-resistance pathways, including the P-glycoprotein, an efflux
73 protein transporting some anti-cancer drugs out of cells (Chen Chen et al., 2010; Cui et al.,
74 2019; Kashyap et al., 2019).

75 The synergistic effect of two drugs is highly dependent on the dosage ratio of these two
76 drugs. However, the difference in pharmacokinetic and biodistribution of the two drugs could
77 prevent their synergistic effect. Nanocarriers encapsulating multiple drugs with different
78 physicochemical and pharmaceutical properties could maintain the optimized synergistic
79 drug ratio in a single carrier *in vivo* up to the point of intracellular uptake in the target cancer
80 cell (Mayer et al., 2006; Tardi et al., 2007, 2009; Gurunathan et al., 2018). The use of a
81 nanocarrier could translate the synergistic effect observed *in vitro* to a preclinical model by
82 maintaining the fixed drug ratio (Harasym et al., 2007). A liposomal formulation
83 (DSPC/DSPG/cholesterol (7:2:1 molar ratio)) encapsulating both cytarabine and daunorubicin
84 in a 5:1 ratio (CPX-351) against acute myeloid leukemia in newly diagnosed patients was
85 recently approved by the FDA and EMA as it showed an improved overall survival versus
86 standard-of-care cytarabine plus daunorubicin chemotherapy (7+3 regimen) (Je et al., 2018;
87 Alfayez et al., 2020). Preclinical *in vitro* testing determined the molar ratio 5:1 as the most
88 effective as it displayed the greatest synergistic effect on a panel of tumor cell lines. The
89 liposomal encapsulation maintained the synergistic drug ratio in plasma for 24 hours after
90 injection and exhibited superior therapeutic activity compared to free drug cocktails,
91 consistent with *in vivo* synergy (Tardi et al., 2009).

92 Co-encapsulation of a flavonoid with an anti-cancer drug has led to a synergistic or additive
93 effect at the tumor site (Fang et al., 2018; Li et al., 2017; Pangen et al., 2018b; Ramasamy
94 et al., 2017; Ray et al., 2017; Wang et al., 2019, p. 20, 2015; Wong and Chiu, 2010, 2011;
95 Zhu et al., 2017), the reversal of resistance (Hu et al., 2016; Meng et al., 2016) and delayed
96 onset of drug resistance by combining agents with different mechanisms of action (Fatma et
97 al., 2016; Jain et al., 2013; Li et al., 2017, 2018; Ramasamy et al., 2017; Sandhu et al., 2017;
98 Wang et al., 2019; Zhu et al., 2017).

99 1.1 Anti-cancer properties of flavonoids

100 Flavonoids are natural polyphenols widely found in fruits, vegetables and tea. They consist of
101 more than 6500 compounds and form one of the largest groups of plant metabolites (Panche
102 et al., 2016).

103 Flavonoids are pleiotropic compounds with several properties such as antioxidant, antifungal,
104 antibacterial, anti-carcinogenic, anti-angiogenic or anti-inflammatory activity (Dayoub et al.,
105 2013; Nagaraju et al., 2013; Adan and Baran, 2015; Ahmad et al., 2016; Carvalho et al.,
106 2017; Samie et al., 2018; Reyes-Farias and Carrasco-Pozo, 2019). They have demonstrated
107 direct cytotoxicity on several tumor cell lines by inhibiting the cell cycle or inducing apoptosis.
108 They also have demonstrated anti-angiogenic effects by targeting the VEGF or the bFGF
109 signaling pathways, as well as by having an activity on matrix metalloprotease or directly on
110 endothelial cells (Su et al., 2005; Touil et al., 2009, 2011; Mirossay et al., 2017). In addition,
111 their anti-inflammatory properties may decrease the chronic inflammation that promotes
112 tumor development, invasion and metastasis pathways (Gupta et al., 2018).

113 1.2 Flavonoids: a need for vectorization

114 Flavonoids are characterized by a common structure of two aromatic rings (A and B) which
115 are linked through a three-carbon oxygenated heterocyclic ring (C) (Figure 1): this is the
116 basic flavane skeleton. They are subdivided into flavonols, flavanols, flavones, flavanones,
117 anthocyanidins and isoflavonoids according to the degree of unsaturation or oxidation of the
118 C-rings, and depending on the carbon on which the B ring is attached to the C ring.

119 Flavonoids can exist as free aglycones and glycosidic conjugates (Bednarek et al., 2003; He,
120 2000). Aglycone flavonoids are hydrophobic molecules, but the glycosylation renders them
121 more water-soluble (Plaza et al., 2014).

122 Depending on their structure, flavonoids are sensitive to light exposure, pH, temperature,
123 solvent type (Jackman et al., 1987). For example, fisetin (FIS), quercetin (QUE), genistein
124 (GEN) and myricetin are degraded in aqueous buffer at elevated temperature and at different
125 rates depending on the pH (Yao et al., 2014; Wang and Zhao, 2016; Chaaban et al., 2017);

126 QUE and FIS are rapidly oxidized and degraded in water (Sokolová et al., 2012; Ramešová
127 et al., 2015); flavonols are sensitive to light exposure and photodegradation is accelerated in
128 the presence of aluminum ions (Smith et al., 2000).

129 Flavonoids can also be subject to rapid metabolism into the intestine by hydrolysis of the
130 glucoside, conjugation and deconjugation of the aglycone skeleton, in addition with
131 elimination of conjugated metabolites by efflux transporters (Chen et al., 2003). There is also
132 a hepatic first pass metabolism where they are conjugated by glucuronidation, sulfation, or
133 methylation or metabolized into smaller phenolic compounds. The aglycon of flavones and
134 flavanols is also degraded by a peroxidative mechanism and the resulting compounds can
135 undergo further degradations by dioxygenase-catalyzed ring-fission reactions (Hinderer and
136 Seitz, 1988).

137 The poor water solubility of most flavonoids is a major drawback for their administration.
138 Combined with their poor absorption, susceptibility to degradation and rapid metabolism are
139 the main factors for their low oral bioavailability (Hinderer and Seitz, 1988; Chen et al., 2003;
140 Crozier et al., 2010).

141 To overcome these limitations, the use of nanocarriers could be a good alternative. Indeed,
142 the encapsulation of flavonoids could increase their apparent solubility and allow their
143 systemic administration. Oral bioavailability may also be enhanced by protection against
144 flavonoid metabolism by the formulation. Therefore, the delivery of flavonoids using
145 nanocarriers has been widely explored, and had led to an increase in their bioavailability and
146 efficacy (Khushnud and Mousa, 2013; Mignet et al., 2013; Seguin et al., 2013; Aiello et al.,
147 2019) (Figure 2).

148 1.3 Co-encapsulation of flavonoids with anti-cancer agents

149 Due to their multiple biological properties, flavonoids have been considered as one of the
150 most promising candidates for combination therapy with anti-cancer drugs in order to
151 increase tumor sensitivity and reduce toxicity (Kikuchi et al., 2019). Co-encapsulating
152 flavonoids with anti-cancer agents could enable delivery of the optimized ratio to the target
153 while protecting the flavonoids from degradation. The use of nanocarriers could also
154 passively target the tumor site using the enhanced permeability and retention (EPR) effect,
155 resulting in drug accumulation in the tumor site and decreased toxicity, as well as potential
156 inhibition of intracellular endocytic uptake mediated drug resistance (Choi et al., 2016). As
157 shown in Figure 3, research in the field of the co-encapsulation of flavonoids with other drugs
158 has increased the last 10 years.

159 The aim of this review is to analyze how to co-encapsulate flavonoids with anti-cancer
160 agents. The first part is dedicated to the formulation/preparation strategy and the challenge
161 of this optimization. The second part reports the *in vitro* experiments to predict the *in vivo*
162 behavior of these nanomedicines and finally their *in vivo* efficacy is discussed in the last
163 chapter.

164 2. Formulation and preparation considerations

165 2.1 Choice of the nanocarrier for co-encapsulation

166 Co-encapsulating a flavonoid with another anti-cancer agent is a challenge. Indeed, the
167 addition of a second drug in the system can create instability. The choice of the nanocarrier
168 is important and depends on the co-encapsulated drugs and the target. As flavonoids are
169 mostly hydrophobic and some anti-cancer drugs are hydrophilic, it is essential to choose a
170 suitable nanocarrier capable of encapsulating both. The different nanocarriers developed to
171 co-encapsulate flavonoids with anti-cancer drugs, as well as their compositions and
172 preparation methods are reported in Table 1. Their characterization methods are reported in
173 Table 2.

174 Polymeric micelles are spherical nanostructures formed by amphiphilic molecules capable of
175 encapsulating lipophilic drugs in their hydrophobic internal core surrounded by the
176 hydrophilic parts enabling their suspension in aqueous medium. They can release their load
177 according to specific stimuli. As they are formed by the self-assembly of block copolymers
178 held together by non-covalent interactions (Savić et al., 2006), the copolymer can be
179 designed to respond to specific stimuli: pH (Gao et al., 2017), temperature (Lee et al., 2015),
180 redox mechanism (Zhou et al., 2017). Several studies chose micelles to co-encapsulate
181 flavonoids with anti-cancer agents, such as silibinin and docetaxel (DTX) (Dong et al., 2017)
182 or QUE and DOX (Ramasamy et al., 2017) with high efficiency.

183 Solid-lipid nanoparticles are submicron-sized lipid emulsions where the liquid lipid (oil) has
184 been replaced by a solid lipid. They can only encapsulate lipophilic drugs, such as baicalin
185 (BAI) (Li et al., 2017). To overcome this limitation, hydrophilic drugs can be conjugated to or
186 complexed with the lipids (Mehnert and Mäder, 2001).

187 Nanoemulsions present the same drawback: oil-in-water nanoemulsion have been proven
188 very effective in delivering lipophilic drugs and increasing the *in vivo* efficacy of anti-cancer
189 agents (Tagne et al., 2008) or improve the bioavailability of flavonoids (Wu et al., 2018), but
190 they encapsulate only drugs with similar lipophilicity, such as baicalein (BCL) with paclitaxel
191 (PTX) (Meng et al., 2016). To overcome this limitation, Pangen *et al* designed
192 water-in-oil-in-water nanoemulsions encapsulating both hydrophilic, amphiphilic and lipophilic

193 compounds (Pangeni et al., 2016, 2018a). Using this strategy, they successfully co-
194 encapsulated QUE and pemetrexed (PMX) (Pangeni et al., 2018b).

195 Liposomes, lipid-polymer hybrid nanoparticles, polymeric nanoparticles and mesoporous
196 silica nanoparticles are all capable of encapsulating both hydrophobic and hydrophilic drugs
197 through different properties.

198 Liposomes are spherical vesicles made of phospholipids associated with other lipids such as
199 cholesterol which stiffens the lipid bilayer and stabilizes it. Their amphiphilic properties allow
200 them to self-assemble and form bilayers. Several studies have reported successful
201 co-encapsulation of flavonoids and anti-cancer drugs in liposomes due to their ability to
202 encapsulate i) hydrophobic drugs such as QUE in their lipid bilayer (Wong and Chiu, 2010),
203 ii) hydrophilic drugs such as doxorubicin hydrochloride (DOX-HCL) or vincristine sulfate (VIN)
204 in their aqueous core (Li et al., 2018; Wong and Chiu, 2010), and iii) amphiphilic drugs at the
205 interface (Hu et al., 2010; Cosco et al., 2011). Moreover, their properties can be altered by
206 modifying their formulation by adding functional groups to phospholipids, other lipids or
207 polymers (Akbarzadeh et al., 2013).

208 Polymeric nanoparticles are formed by amphiphilic copolymers self-assembling in water into
209 nanoparticles. They usually present better stability, sharper size distribution and more
210 controlled drug-release profile than liposomes (Hu et al., 2010). Most of the reviewed studies
211 chose this nanosystem to co-encapsulate flavonoids and anti-cancer drugs (Table 1). They
212 typically encapsulate hydrophobic drugs, such as QUE and tamoxifen (TMX) (Jain et al.,
213 2013), BCL and PTX (Wang et al., 2015) or DOX and icaritin (ICA) (Yu et al., 2020), but are
214 able to encapsulate hydrophilic drugs by conjugation to the polymer or by attachment to the
215 surface of the nanoparticles (Pan et al., 2019).

216 Lipid-polymer hybrid nanoparticles are multifunctional drug delivery platforms, which
217 combines the mechanical advantages of polymeric core capable of encapsulating lipophilic
218 drugs and the biomimetic advantages of the phospholipid shell in a single platform (Hadinoto
219 et al., 2013). For example, they have been used to co-encapsulate GEN and PTX (Mendes
220 et al., 2014).

221 Mesoporous silica nanoparticles are inorganic nanoparticles that can be functionalized. Their
222 highly controlled porous structure and functionalization enable them to encapsulate both
223 hydrophobic and hydrophilic drugs (Narayan et al., 2018). They were able to co-encapsulate
224 flavonoids with lipophilic anti-cancer agents (Murugan et al., 2016; Fang et al., 2018).

225

Table 1. Types, formulation, preparation method and targets of nanocarriers co-encapsulating a flavonoid with an anti-cancer agent.

Flavonoid	Co-encapsulated drug	Flavonoids/drug encapsulation DL or EE (%)	Optimal wt ratio FLA/drug	Nanocarrier composition	Preparation method	Purification method	Formulation or process optimization	Administration route	Cancer	References
<i>Micelles</i>										
BAI	CUR	DL BAI : 3.50 ± 0.34 CUR : 7.46 ± 1.70	3.5:7.5*	quercetin dithiodipropionic acid oligomeric hyaluronic acid mannose ferulic acid polymer	Solvent-exchange	Centrifugation		Parenteral	NSCLC	(Wang et al., 2019)
QUE	DOX	Active loading capacity QUE: ~18 DOX: ~24	1:5	Poly(phenylalanine)-b-poly(L-histidine)-b-poly(ethylene glycol)	Solvent-exchange	Ultrafiltration		Parenteral	Squamous cell carcinomas	(Ramasamy et al., 2017)
SIL	DTX	DL SIL: 4.1 ± 0.2 DTX: 2.8 ± 0.3	6:4*	polyethylene glycol-blockpoly[(1,4-butanediol)-diacrylate-β-N,N-diisopropylethylenediamine]	Thin-film hydration	Dialysis		Parenteral	Metastatic breast cancer	(Dong et al., 2017)
<i>Nanoemulsions</i>										
BCL	PTX	EE BCL: 97.9 PTX: 97.1	1:1	Oil phase : Soybean oil and medium chain triglycerides Aqueous phase: Soybean lecithin, poloxamer 188, glycerol	High pressure homogenization	Ultracentrifugation	Preparation of complex: BCL-PL and PTX-cholesterol	Parenteral	Breast cancer	(Meng et al., 2016)
QUE	PMX	Non specified	2:1	Surfactant : Labrasol, Tween 80, Oil phase: Labrafil M 1944 CS Cremophor EL:PEG 400 Deionized water	Low-energy spontaneous emulsification		Complexation of PMX with DCK Screening of surfactants and co-surfactants Wt ratio of surfactants Concentration of drugs Pseudo ternary diagram QbD based model	Oral	Lung carcinoma	(Pangeni et al., 2018b)
NG	TMX	Non specified	Non specified	corn oil-lipid, labrasol and transcutol P	Mixing (SNEDDS)			Oral	Breast cancer	(Sandhu et al., 2017)
<i>Solid lipid nanoparticles</i>										
BAI	DTX	DL BAI: 4.9 ± 0.6 DTX: 8.3 ± 0.6	37:63*	Soya lecithin, glyceryl monostearate Tf-PEG-hz-GMS, poloxamer 188	Emulsification	Centrifugation + filtration		Parenteral	Lung cancer	(Li et al., 2017)
<i>Liposomes</i>										
QUE	TMZ	DL QUE: 23.42 ± 2.17 TMZ: 15.87 ± 1.96 EE*	6:4*	Tween 80, poloxamer 188, DSPE-PEG2000 Glyceryl behenate, soy lecithin, cholesterol	Emulsification- evaporation and low temperature curing	Dialysis		Parenteral	Glioma	(Hu et al., 2016)
QUE	VIN	QUE: 78.5 VIN: 78.3	1:2	Egg sphingomyelin, cholesterol,, ceramide-PEG2000	Thin-film hydration Loading of VIN with ionophore-mediated proton gradient	Size-exclusion chromatography	Optimization of the cholesterol ratio	Parenteral	Trastuzumab-insensitive breast tumor	(Wong and Chiu, 2010, 2011)
SIL	GCA	EE SIL: 24.37 GCA: 68.78		DPPC, cholesterol, PEG2000-DSPE	Thin-film hydration	Dialysis		Non specified	Hepatocellular carcinoma	(Ochi et al., 2016)
SLB	DOX-HCL	EE SLB: 93.07 ± 3.07 DOX-HCL: 95.74 ± 9.09	3:1	DSPE-PEG-cholic acid, cholesterol, phospholipids	Ethanol injection Loading of DOX-HCL with ammonium sulfate gradient	Ultrafiltration		Oral	Hepatocellular carcinoma	(Li et al., 2018)
<i>Lipid-polymer hybrid nanoparticles</i>										

QUE	VIN	LE QUE: 5.1 ± 0.9 VIN: 12.3 ± 2.5	1:1	PLGA, cholesterol, stearic acid, DSPE-PEG2000	Nanoprecipitation	Ultrafiltration		Parenteral	Non-Hodgkin's lymphoma	(Zhu et al., 2017)
GEN	PTX	EE GEN: 97.99 ± 2.90 PTX: 97.80 ± 2.21	12:0:2	PLGA + Capric/caprylic triglyceride Pluronic F68 and F127 Phosphatidylcholine	Emulsification- evaporation Thin-film hydration	Filtration		Parenteral	Ehrlich Ascites Tumor	(Mendes et al., 2014)
<i>Polymeric nanoparticles</i>										
QUE	CUR	Similar entrapment								
QUE	ASP	QUE: 6.2	4.4:1:4.6	Chitosan- sodium hexametaphosphate	Nanoprecipitation	Dialysis			Colorectal cancer	(Ray et al., 2017)
QUE	CUR + ASP	CUR: 1.5 ASP: 6.5	*							
QUE	TMX	EE QUE: 68.60±1.58 TMX: 67.16±1.24	2:1	PLGA	Emulsification- evaporation	Centrifugation	pH, type and concentration of PLGA, type and concentration of stabilizers, drugs loading ratio	Oral	Estrogen receptor positive breast cancer	(Jain et al., 2013)
QUE	DOX	DL QUE: 7.9 DOX: 3.6	6.9:3:1	Biotin-decorated poly(ethylene glycol)-b-poly(ε-caprolactone)	Thin-film hydration	Centrifugation		Parenteral	Breast cancer	(Lv et al., 2016)
BCL	PTX	EE BCL: 87.6 ± 3.1 PTX: 90.8 ± 2.9	5:1	Folate-valine-PTX Hyaluronic acid-lysine-BCL PLGA, poloxamer 188 PLGA, poly-vinyl alcohol	Nanoprecipitation	Filtration		Parenteral	Lung cancer	(Wang et al., 2015)
QUE	ETO	EE QUE: non specified ETO: 62.46 ± 1.22	1:10		Emulsification solvent evaporation	Centrifugation	O/W phase ratio polymers concentration Sonication time Drug:polymer ratio ETO:QUE ratio	Oral	Breast cancer	(Fatma et al., 2016)
ICA	DOX	DL ICA: 2.1 DOX: 10.8	3:1	PLGA-PEG, PLGA-PEG-aminoethyl anisamide	Nanoprecipitation	Ultrafiltration	ICA:DOX molar ratio	Parenteral	Hepatocellular carcinoma	(Yu et al., 2020)
EGCG	PTX	EE EGCG: 76.8 ± 9.1 PTX: 95.7 ± 7.3		PLGA, casein	Emulsion- precipitation	Centrifugation	Polymer/PTX ratio Casein/EGCG ratio	Parenteral	Breast tumor	(Narayanan et al., 2014)
<i>Mesoporous silica nanoparticles</i>										
QUE	DOX	Maximal DL QUE: 29.7 DOX: 32.6	1:1	Hyaluronic acid-silica	Nanoprecipitation	Centrifugation		Parenteral	Gastric carcinoma	(Fang et al., 2018)
QUE	TPT	DL QUE: 1,2 TPT: 1,8	4:6*	Silica, arginine-glycine-aspartic acid peptide, poly(acrylic) acid-chitosan	Nanoprecipitation	Centrifugation			Breast cancer (triple negative and MDR)	(Murugan et al., 2016)

227 *Calculated using the drug loading reported

228 ASP = aspirin, BAI = baicalin, BCL = baicalein, CUR = curcumin, DCK = N^ε-deoxycholy-L-lysyl-methylester, DL = Drug loading, DOX = doxorubicin base, DOX-HCL = doxorubicin hydrochloride, DSPE-PEG2000 = 1,2-
229 distearoyl-sn-glycero-3-phosphoethanolamine-N-[methoxy(polyethylene glycol)-2000], DTX = docetaxel, EE = encapsulation efficiency, EGCG = (-)-Epigallocatechin gallate, ETO = etoposide, FLA = flavonoids, GCA =
230 glycyrrhizic acid, GEN = genistein, ICA = icaritin, NG = naringenin, NSCLC = non small cell lung cancer, PEG = polyethylene glycol, PLGA = Poly (lactic-co-glycolic acid), PMX = pemetrexed, PTX = paclitaxel, QbD =
231 quality by design, QUE = quercetin, SIL = silibinin, SLB = silybin., SNEDDS = self-nano-emulsifying drug delivery systems, TMX = tamoxifen, Tf-PEG-hz-GMS = transferrin-polyethylene glycol-hydrazone-lyceryl
232 monostearate, TMZ = temozolomide, TPT = topotecan, VIN = vincristine.

Table 2. Characteristics and characterization methods of nanocarriers co-encapsulating a flavonoid with an anti-cancer agent.

Flavonoid / co-encapsulated drug	Size (nm)	PDI	Minimal requirements Morphology	Zeta potential (mV)	Dosage of flavonoid (direct or indirect)	Additional characterization methods	References
<i>Micelles</i>							
BAI/CUR	121.0 ± 15	0.129	Spherical (TEM)	-20.33 ± 4.02	HPLC (UV detection) (Direct method)	Proton nuclear magnetic resonance	(Wang et al., 2019)
QUE/DOX	82.0 ± 3.4		Spherical (TEM, AFM)	-20	HPLC (UV detection) (Indirect method)	Proton nuclear magnetic resonance Gel permeation chromatography Critical micellar concentration X-ray diffractometry Fourier transform infrared spectroscopy	(Ramasamy et al., 2017)
SIL/DTX	85.3 ± 0.4	0.190 ± 0.1	Spherical (TEM)		HPLC (UV detection) (not specified)	Proton nuclear magnetic resonance u Matrix-assisted laser desorption-ionization – time of flight mass spectrometry Nile red assay	(Dong et al., 2017)
<i>Nanoemulsions</i>							
BCL/PTX	170.5 ± 6.5	0.113 ± 0.005	Spherical (TEM)	-42.4 ± 3.7	HPLC (indirect method)		(Meng et al., 2016)
QUE/PMX	13.2 ± 0.132)	0.095 ± 0.015	Spherical (TEM)	-3.99 ± 1.11	Non specified		(Pangeni et al., 2018b)
NG/TMX	52 – 73		Spherical (TEM)		Non specified	Self-emulsification time	(Sandhu et al., 2017)
<i>Solid lipid nanoparticles</i>							
BAI/DTX	135.5 ± 4.7	0.16 ± 0.05	Spherical (TEM)	-31.6 ± 3.5	HPLC (UV detection)	Proton nuclear magnetic resonance Colloidal stability	(Li et al., 2017)
<i>Liposomes</i>							
QUE/TMZ	196.5 ± 47.3	0.32 ± 0.09 (DLS)	Spherical (TEM)	30.5 ± 6.9	HPLC (UV detection) (direct method and indirect) UV-vis (direct method)	UV-Vis spectra Fourier transform infrared spectroscopy	(Hu et al., 2016)
QUE/VIN	135.9 ± 12.	0.161 ± 0.032 (DLS)					(Wong and Chiu, 2011, 2010)
SIL/GCA	46.3 ± 0.4		Spherical (SEM, TEM)	-23.25 ± 0.83	HPLC (UV detection) (direct method)	Fourier transform infrared spectroscopy	(Ochi et al., 2016)
SLB/DOX-HCL	97.0 ± 2.2	0.239 ± 0.026 (DLS)	Spherical (TEM)		HPLC (UV detection) (direct method)	Stability in SGF and SIF (12 hours) Colloidal stability in plasma	(Li et al., 2018)
<i>Lipid-polymer hybrid nanoparticles</i>							
QUE/VIN	115.7 ± 5.5	0.22 ± 0.05	Spherical (TEM)	-36.4 ± 3.5	HPLC (VIN) UV-vis (QUE) (direct method)	Colloidal stability	(Zhu et al., 2017)
GEN/PTX	151.5 ± 5.6	0.17 ± 0.03	Spherical (TEM)		HPLC (UC detection) (direct method)	Nanoparticles tracking analysis Multiple light scattering	(Mendes et al., 2014)
<i>Polymeric nanoparticles</i>							
QUE/CUR	118 ± 5.6		Spherical (TEM, SEM)		UV-vis (direct method)		(Ray et al., 2017)
QUE/ASP	128 ± 0.9						
QUE/CUR/ASP	92 ± 0.7	0.12					
QUE/TMX	185.3 ± 1.20	0.184 ± 0.004			HPLC (UV detection) (direct method)	Stability in SGF and in SIF X-ray diffractometry Differential scanning calorimetry	(Jain et al., 2013)
QUE/DOX	105.8 ± 1.4	0.168 ± 0.023	Spherical (TEM)	-9.56 ± 1.80	HPLC (UV detection) (Direct method)		(Lv et al., 2016)

BCL/PTX	91.8 ± 2.3	0.1 ± 0.03	Spherical (TEM)	+3.3 ± 0.6	HPLC (UV detection) (not specified)	Proton nuclear magnetic resonance Fourier transform infrared spectroscopy	(Wang et al., 2015)
QUE/ETO	254.3	0.11	Spherical (TEM, SEM)		HPLC (UV detection) (direct method)		(Fatma et al., 2016)
ICA/DOX	~138		Spherical (TEM)	~3	HPLC (Not specified)		(Yu et al., 2020)
EGCG/PTX	~100 (TEM) 230 ± 27 190 ± 12 (TEM)	0.18 (SEM)	Spherical (SEM, TEM)	-41 ± 3.4	HPLC (UV detection) (not specified)	Fourier transform infrared spectroscopy Raman in confocal microscopy BCA protein estimation assay Degradation of casein Colloidal stability	(Narayanan et al., 2014)

Mesoporous silica nanoparticles

QUE/DOX	101.6 ± 3.21	0.123 ± 0.06	Spherical (TEM)	-28.56 ± 2.31	UV-vis (indirect method)	Fourier transform infrared spectroscopy Colloidal stability	(Fang et al., 2018)
QUE/TPT	72.9	0.03	Spherical (SEM,TEM)	+42.80	UV-vis (indirect method)	Thermogravimetric analysis Nitrogen adsorption/desorption isotherm Fourier transform infrared spectroscopy	(Murugan et al., 2016)

234 ASP = aspirin, BAI = baicalin, BCL = baicalein, CUR = curcumin, DOX = doxorubicin base, DOX-HCL = doxorubicin hydrochloride, DTX = docetaxel, EGCG = (-)-epigallocatechin gallate, ETO = etoposide, GCA =
235 glycyrrhizic acid, GEN = genistein, HPLC = high performance liquid chromatography, ICA = icaritin, NG = naringenin, PMX = pemetrexed, PTX = paclitaxel, QUE = quercetin, SEM = scanning electron microscopy, SGF
236 = simulated gastric fluid, SIF = simulated intestinal fluid, SIL = silibinin, SLB = silybin, TEM = transmission electron microscopy, TMX = tamoxifen, TMZ = temozolomide, TPT = topotecan, VIN = vincristine.

237

238 2.2 Optimization of the formulation and the process of preparation

239 2.2.1. Nanocarrier size

240 Once the drugs and carriers are chosen, several investigations must be conducted to
241 optimize the formulation and process. Excipients and process are usually chosen with these
242 critical parameters in mind: nanocarrier size and polydispersity (PDI), and drug loading. Zeta
243 potential will not be discussed as it was mostly used to characterize the final nanocarriers or
244 to assess the influence of nanocarrier surface modifications more than the influence of the
245 co-encapsulation.

246 The size of the nanocarriers is of great importance as it influences their *in vivo* behavior. The
247 pharmacokinetics of nanocarriers can be modified by a diameter under 5 nm, where they will
248 be excreted by renal excretion (Choi et al., 2007), or by a diameter above 100 nm where they
249 will be eliminated by the mononuclear phagocytic system more rapidly than with a diameter
250 under 100 nm (Moghimi et al., 2001). Their internalization into cells (endocytosis) and their
251 accumulation in the tumor *via* the EPR effect are also affected. The ideal diameter of a
252 nanocarrier used for parenteral injection should be less than 200 nm (Peer et al., 2007). This
253 size can be achieved directly as a function of the formulation and preparation process, or a
254 size calibration may be required. There are many methods to measure the size of the
255 nanocarriers: indirect methods such as light scattering (LS) or tunable resistive pulse
256 sensing, and direct method such as electron microscopy (transmission electron microscopy
257 (TEM) or scanning electron microscopy (SEM)), field flow fractionation and capillary
258 electrophoresis. A combination of several methods, including a microscopic one to assess
259 the morphology, is highly recommended (Gaumet et al., 2008). Most of the studies reviewed
260 here assessed the size and polydispersity using dynamic light scattering (DLS) and TEM or
261 SEM, and presented spherical particles with diameter under 200 nm.

262 Co-encapsulating two agents into one nanocarrier can sometimes increase its diameter.
263 Ramasamy *et al* reported an increase of the co-loaded micelles' size compared to blank
264 micelles identified by TEM (Ramasamy et al., 2017). Hu *et al* evidenced an increase in
265 hydrodynamic diameter and PDI of liposomes co-encapsulating QUE and temozolomide
266 (TMZ) (Hu et al., 2016). Moreover, Narayanan *et al* identified by DLS and TEM an increase
267 in size with the casein shell formation around the poly(lactic-co-glycolic acid) (PLGA)
268 nanoparticles as well as with drug loading, from 168 ± 18 nm to 230 ± 27 nm (Narayanan et
269 al., 2014). Mendes *et al* encapsulated GEN by coating the PTX-PLGA-nanoparticles with a
270 lipid bilayer incorporating GEN, which led to an increase in the size of the lipid-polymer
271 hybrid nanoparticles (Mendes et al., 2014). On the contrary, other studies showed no impact
272 of the co-encapsulation on the hydrodynamic diameter of nanocarriers compared to

273 unloaded nanocarriers (Li et al., 2017; Zhu et al., 2017; Pangen et al., 2018b) or
274 single-loaded nanocarriers (Wang et al., 2015; Lv et al., 2016; Li et al., 2017; Zhu et al.,
275 2017). It should be noted that although some formulation optimization can lead to a better
276 drug entrapment, it can also lead to an increase in nanocarrier size. For example, Jain *et al*
277 showed that even if the use of PVA 1% as a surfactant increased the entrapment efficiency,
278 the size was above than 200 nm and the PDI unacceptable, while the loading ratio of TMX
279 and QUE and their total amount to be incorporated had no impact in term of size (Jain et al.,
280 2013). It is difficult to discern a trend from these results: if the size never decreases after co-
281 encapsulation, it can remain the same as after single-encapsulation or as empty nanocarrier.
282 Co-encapsulation did not seem to have an impact in term of size compared to single-
283 encapsulation, but few studies have compared both (Wang et al., 2015; Lv et al., 2016; Hu et
284 al., 2016; Li et al., 2017; Zhu et al., 2017). The addition of a drug incorporating shell or
285 bilayer around nanoparticles can lead to an increase in size (Mendes et al., 2014; Narayanan
286 et al., 2014).

287 2.2.2. Drug loading

288 Drug loading is directly impacted by the chosen process and purification method. After
289 preparation, a purification step is required to remove non-encapsulated drugs from the
290 nanocarrier suspension. At this point, determination of the drug loading in the system is
291 possible either by assaying the drug still encapsulated in the system after a step of disruption
292 of this system (direct method), or by assaying the non-encapsulated drug and deducing the
293 content of the still encapsulating drug (indirect method). This enable the determination of the
294 encapsulation efficiency, which is the amount of entrapped drug divided by the total amount
295 of drug added in the preparation, and the drug loading, which is the amount of total
296 entrapped drug divided by the total nanoparticle weight, both expressed in percentage. Drug
297 loading seems to be the better parameter to compare the encapsulation in different
298 nanocarriers, but some publications presented only the encapsulation efficiency. Since
299 flavonoids are mostly hydrophobic, the choice of the purification method depends on this. For
300 example, in liposomes, hydrophobic flavonoids are located inside the lipid bilayer, near the
301 water/lipids interface (Mohapatra and Mishra, 2011; Mignet et al., 2013) and can leak from
302 the liposomes when aggressive methods are used such as ultrafiltration or centrifugation. In
303 contrast, when flavonoids are covalently bound or within a nanoparticle, they are less prone
304 to leakage with these methods. The different purification strategies used to prepare
305 nanocarriers co-encapsulating flavonoids and anti-cancer agents were mainly centrifugation
306 (Fang et al., 2018; Fatma et al., 2016; Jain et al., 2013; Li et al., 2017; Lv et al., 2016; Meng
307 et al., 2016; Murugan et al., 2016; Narayanan et al., 2014; Wang et al., 2019), dialysis (Dong
308 et al., 2017; Hu et al., 2016; Ochi et al., 2016; Ray et al., 2017), ultrafiltration (Li et al., 2018;

309 Ramasamy et al., 2017; Yu et al., 2020; Zhu et al., 2017) and size-exclusion chromatography
310 (Wong and Chiu, 2011, 2010). We can discuss the efficiency of centrifugation and
311 ultrafiltration as methods to separate non-encapsulated hydrophobic drugs from
312 nanocarriers. Indeed, after centrifugation or ultrafiltration, the nanocarriers are usually found
313 in the centrifugation pellet (except for micelles found in the supernatant) and resuspended
314 after the supernatant elimination. However, the non-encapsulated hydrophobic drugs would
315 also precipitate in the pellet and not be separated. Most studies report several washing steps
316 of the nanoparticles that could help remove the likely precipitated flavonoid (Table 1).
317 However, the washing medium was water (Fatma et al., 2016; Murugan et al., 2016; Zhu et
318 al., 2017) or not defined (Jain et al., 2013; Narayanan et al., 2014; Li et al., 2018).

319 Drug loading is assessed after purification. As discussed in section 1.2, flavonoids are
320 reactive and could be degraded during some preparation steps, depending on the pH or the
321 temperature used (Gaber et al., 2017). An analytical method able to monitor the apparition of
322 impurities, such as high performance liquid chromatography (HPLC) is highly recommended
323 (Tsao, 2010; Corradini et al., 2011). Flavonoids can be detected by UV. Indeed, due to their
324 polyphenolic structure, most flavonoids present two absorption bands in the UV spectrum:
325 band I between 320 and 385 nm and band II between 250 and 285 nm which allow their UV
326 detection. Their maximum absorption wavelengths differ according to the functional groups
327 attached to the skeleton (Kumar and Pandey, 2013). As shown in Table 2, most studies used
328 reverse phase HPLC coupled with a UV detector to assay the drugs. However, some used
329 an indirect method to estimate drug loading. The direct method, consisting of the direct
330 determination of flavonoids remaining in nanocarriers, should be preferred to the indirect
331 method that could overestimate the loading if some degradation occurred during the process.

332 Co-encapsulating flavonoids with another drug may impact the loading of both drugs. Indeed,
333 the two drugs might be in competition in the site of incorporation, or one may destabilize the
334 structure needed for the other.

335 All type of nanocarriers described here have been used to successfully co-encapsulate
336 lipophilic drugs, with some studies reporting formulation or process optimization. Jain *et al*
337 compared the impact of the initial TMX:QUE ratio (1:1, 1:2 and 1:3) introduced for the
338 preparation of co-loaded polymeric nanoparticles. Increasing the proportion of QUE
339 introduced into the preparation did not impact the TMX loading, but QUE loading decreased
340 significantly when the ratio TMX:QUE was 1:3 (from 4.10 ± 0.03 to $2.95 \pm 0.23\%$), indicating
341 that the best entrapment was achieved for an initial TMX:QUE ratio of 1:2 (Jain et al., 2013).
342 Other teams co-encapsulating flavonoids with another lipophilic drug checked that the
343 encapsulation of each drug was the same when they were either encapsulated alone or

344 co-encapsulated in the nanocarriers; however, the path to the optimized formulation was
345 never reported (Mendes et al., 2014; Wang et al., 2015; Lv et al., 2016; Meng et al., 2016;
346 Hu et al., 2016; Li et al., 2017). Yu *et al* observed that co-encapsulation of ICA and DOX
347 increased the DOX loading (loading capacity from 8.3% encapsulated alone to 10.8%
348 encapsulated with ICA) ; they hypothesized a π - π stacking interaction but did not investigate
349 it (Yu et al., 2020). Pangeni *et al* optimized the concentrations of PMX complexed with N^α-
350 deoxycholy-L-lysyl-methylester (DCK) (PMX/DCK) and QUE introduced in the
351 water-in-oil-in-water nanoemulsion by determining the maximum drug loading capacity with
352 the minimum concentration of surfactants and co-surfactants introduced able to produce
353 transparent nanoemulsion (Pangeni et al., 2018b). Fatma *et al* optimized the
354 co-encapsulation of etoposide (ETO) and QUE in nanoparticles by evaluating the
355 drug-polymer ratio and drug partitioning in the organic phase but the data were not reported
356 (Fatma et al., 2016). These two studies report detailed results on the choice and proportions
357 of the surfactant and cosurfactant to obtain the best nanoemulsion (Pangeni et al., 2018b) or
358 on the influence of the excipients for a single-drug encapsulation (Fatma et al., 2016), but fail
359 to report the loading of the co-encapsulated drugs.

360 The difficulty increases if the co-encapsulated drug and the flavonoid present different
361 physicochemical characteristics. Nanocarrier formulations optimized for flavonoid
362 incorporation and stabilization might not be optimal for the other drug. Formulation strategies
363 including a compromise might be necessary and the co-encapsulation effect must be
364 explored. For example, micelles can only encapsulate lipophilic drugs. Ramasamy *et al* had
365 to convert DOX-HCL into doxorubicin base (DOX) in order to incorporate it into the micelles.
366 In liposomes, flavonoids are inserted into the lipid bilayer, next to the polar head (Mignet et
367 al., 2013), and can therefore destabilize the bilayer. It is important to study the interaction of
368 flavonoids with the lipid bilayer and to characterize the influence of their incorporation. Wong
369 *et al* optimized the best cholesterol ratio in the bilayer to co-encapsulate QUE and VIN by
370 determining the encapsulation of each drug as a function of the cholesterol molar ratio
371 (Wong and Chiu, 2010). To prevent destabilization, Murugan *et al* formulated pH-responsive
372 mesoporous silica nanoparticles loaded with hydrophilic topotecan (TPT) via electrostatic
373 interactions in the pores; to stabilize QUE, co-loaded with TPT, they conjugated it to the
374 pH-responsive polymer coating the nanoparticles (Murugan et al., 2016). They confirmed the
375 TPT encapsulation by thermogravimetric analysis and desorption curves, and the QUE
376 conjugation by Fourier Transform InfraRed spectroscopy (FTIR). Narayanan *et al* designed
377 PLGA–casein polymer–protein hybrid nanocarriers co-encapsulating (-)-epigallocatechin
378 gallate (EGCG) and PTX. PTX was entrapped in the polymeric core while EGCG was
379 retained by the protein shell. They optimized the PTX:PLGA:EGCG:casein ratio, and

380 confirmed that precipitating casein around the PTX-loaded PLGA nanoparticles did not affect
381 PTX entrapment (Narayanan et al., 2014).

382 Other teams encapsulated both hydrophobic flavonoid and hydrophilic drug using the
383 different compartments of the nanoparticles without describing detailed investigations. Li *et al*
384 designed liposomes co-encapsulating the hydrophobic silybin (SLB) in the lipid bilayer and
385 the hydrophilic DOX-HCL in the aqueous core at an optimized ratio 3:1 (Li et al., 2018). Zhu
386 *et al* encapsulated both QUE and VIN in lipid-polymeric nanocarriers composed of PLGA,
387 cholesterol, stearic acid and DSPE-PEG2000 (Zhu et al., 2017). Ray *et al* formulated
388 spherical cross-linked chitosan-sodium hexametaphosphate nanoparticles encapsulating
389 three drugs: QUE, curcumin (CUR) and aspirin (ASP). They also prepared two-drug loaded
390 nanoparticles (Ray et al., 2017). For these three studies, no formulation optimization and/or
391 preliminary testing was reported. Instability potentially caused by the co-encapsulation was
392 not reported, nor during the process of preparation and neither during the storage.

393 Few studies reported the impact of co-encapsulation in term of drug loading or size, and
394 gave only results on optimization of the nanocarriers taking into account the
395 co-encapsulation. It is regretful that the influence and the validation of the purification step
396 was never reported.

397 Co-encapsulating two drugs together might lead to physicochemical interactions between
398 them, especially if both are loaded in the same compartment of the nanocarriers. Some
399 studies specified that the drugs, due to their different hydrophobicity, are loaded in two
400 different phases of the nanoemulsion (Pangeni et al., 2018b), or one into the lipidic bilayer
401 and the other one into the aqueous core of the liposomes (Li et al., 2018). Similarly, core-
402 shell nanoparticles can be loaded in their two compartments: one in the polymeric core and
403 the other one in the phospholipidic bilayer coating (Mendes et al., 2014) or the casein shell
404 (Narayanan et al., 2014). However, only Murugan *et al* experimentally demonstrated the
405 localizations of one drug adsorbed on the pores of the mesoporous silica nanoparticles and
406 the other on the outer layer (Murugan et al., 2016). No team studied the possible
407 physicochemical interactions between the two drugs, even if they had similar lipophilic
408 properties and consequently may be found in the same compartment of the nanocarrier.

409 From Table 1 and Table 2, we can observe that the minimal characterization of the
410 nanocarriers are the same for co-encapsulation or single encapsulation: size distribution,
411 surface charge, morphology and drug loading. Some characterizations might be interesting
412 to apprehend the capacity of the system to co-encapsulate efficiently the two drugs. For
413 instance, a lipid bilayer permeation study after incorporation of the flavonoid into the

414 liposome could be performed to assess whether this may lead to the leakage of the
415 hydrophilic drug (Mingeot-Leclercq et al., 2001; Bensikaddour et al., 2008).

416 2.3 Shelf-stability of the co-encapsulating nanocarriers

417 Co-encapsulating a flavonoid with another anti-cancer agent can imply encapsulating two
418 drugs with potential different physicochemical properties. Thus, a compromise in the
419 formulation might have to be chosen, leading to an optimal formulation for both drugs, but not
420 necessarily the best for the single-encapsulation of each drug. This can lead to a time-
421 dependent instability of the formulation, such as leaking of the drugs outside the
422 nanocarriers, aggregation of the nanocarriers, oxidation of the lipids, etc. Storage stability
423 must be studied at least in term of preservation of size, polydispersity and drug
424 encapsulation. Indeed, this information is crucial to determine the maximum delay between
425 preparation and cell or *in vivo* experiments. It also provides data for the eventual mass-
426 production and commercialization of the formulation, for which a consequent storage stability
427 is mandatory.

428 Few studies reported the shelf-stability of their formulations. The results are summarized in
429 Table 3. The conditions of these stability studies were heterogeneous in terms of duration,
430 from 1 month to 6 months, temperature, relative humidity and storage form (in buffer, plasma
431 or lyophilized) and did not refer to the standardized conditions described in the ICH Q1A(R2)
432 guidelines. The optimized formulations showed good size stability, but even fewer
433 publications studied the drug leakage.

434 Liquid nanoemulsions appear to be stable for several months at 4°C in term of size, PDI and
435 drug retention; they are successful in retaining either lipophilic (QUE, BCL, PTX) or
436 amphiphilic (PMX) drugs: less than 1% drug leakage in 6 months at 4°C for BCL/PTX
437 nanoemulsions (Meng et al., 2016) and less than 3% of drug leakage after 3 months at 25°C
438 for QUE/PMX nanoemulsions (Pangeni et al., 2018b). It is regrettable that too few studies
439 have investigated the shelf stability for other types of nanocarriers. Suspensions of co-
440 encapsulating liposomes showed leakage of either the lipophilic SIL or the hydrophilic GCA
441 over time, with better retention of the lipophilic drug: 22% of SIL and 61% of GCA leaked
442 from the liposomes after 3 months of storage at 4°C (Ochi et al., 2016). This result is not
443 surprising as lipids can suffer degradation (oxidation, hydrolysis) leading to the leakage of
444 encapsulated drugs. This is why some commercialized liposomal formulations, such as
445 Ambisome® or Vyxeos®, are freeze-dried (Chengjun Chen et al., 2010). Freeze-drying was
446 the method chosen by Jain *et al* to retain the lipophilic QUE and TMX inside nanoparticles,
447 but there was no comparison with the suspension shelf stability (Jain et al., 2013). Because
448 of the lack of shelf stability studies, it is impossible to determine a type of nanocarrier or a

449 process that guarantees the best retention of a flavonoid with an anti-cancer drug inside a
 450 nanocarrier.

451 Table 3. Shelf-stability in term of size and encapsulation of nanocarriers co-encapsulating a
 452 flavonoid with an anti-cancer agent.

Flavonoid / co- encapsulated drug	Type of nanocarrier	Storage stability			References
		Conditions	Size (nm) (PDI)	Drug leakage (%)	
QUE/DOX	Micelles	1 month, 4°C PBS pH 7.4 Serum media	Stable Stable	- -	(Ramasamy et al., 2017)
BCL/PTX	Nanoemulsion	6 months; 4°C	169.5 ± 6.0 (0.115 ± 0.001)	BCL < 1% PTX < 1%	(Meng et al., 2016)
QUE/PMX	Nanoemulsion	3 months 25 ± 2°C (60 ± 5% relative humidity)	Stable	<3% release	(Pangeni et al., 2018b)
QUE/VIN	Liposomes	180 days, 4°C	Stable	-	(Wong and Chiu, 2011, 2010)
SIL/GCA	Liposomes	3 months, 4°C	58.2 ± 3.8	Release SIL: 22%* GCA: 61%*	(Ochi et al., 2016)
QUE/TMX	Polymeric nanoparticles	25±2°C RH 55 ± 2% 3 months lyophilized	Stable	Stable	(Jain et al., 2013)

453 *BCL = baicalein, DOX = doxorubicin base, GCA = glycyrrhizic acid, PMX = pemetrexed, PTX = paclitaxel, QUE = quercetin, SIL*
 454 *= silibinin, TMX = tamoxifen, VIN = vincristine.*

455 *calculated using EE at day 0 and month 3

456 3. *In vitro* prediction of the *in vivo* behavior of the co-encapsulating nanocarrier

457 To formulate the best nanomedicines, some *in vitro* experiments in biological medium can be
 458 performed to evaluate the behavior of the co-loaded nanocarriers: colloidal stability in cell
 459 culture medium, *in vitro* release, and calculation of the combination index evaluating the
 460 synergism during cell culture experiments. Those assays could permit to approach the *in vivo*
 461 behavior by combining the identification of the best ratio between the two drugs to obtain a
 462 synergistic or additive activity and verification of a similar release of both from the
 463 nanocarrier to always maintain this optimized ratio.

464 3.1 Colloidal stability in cell culture media

465 Colloidal stability of the nanocarriers co-encapsulating a flavonoid and an anti-cancer agent
 466 could be evaluated in plasma for a parenteral administration or in simulated intestinal fluid
 467 (SIF) and gastric fluid (SGF) in case of an oral route.

468 To predict its stability in plasma, only size was usually studied in 10% fetal bovine serum
 469 (FBS) in phosphate buffer saline (PBS) (Li et al., 2017; Zhu et al., 2017), in 20% serum in
 470 buffer (Fang et al., 2018) or in rat serum (Li et al., 2018) at 37°C. All these studies
 471 evidenced no size modification and no aggregation with duration of studies ranging from 12

472 hours (Li et al., 2018) to 24 hours (Zhu et al., 2017), 48 hours (Fang et al., 2018) or 72 hours
473 (Li et al., 2017). Sometimes, the drug encapsulation were also monitored and showed good
474 retention of the encapsulated drugs with no change in the encapsulation efficiency. This is
475 surprising as there is an *in vitro* release of about 20% of the encapsulated drugs in aqueous
476 buffer at 37°C: this might be explained by the fact that the dilutions for plasma stability
477 assays are lower than those for *in vitro* release ones (1/10 versus 1/50 (Li et al., 2018) or
478 unspecified versus 1/25 (Zhu et al., 2017)). Narayanan *et al* suspended EGCG and PTX
479 co-loaded nanoparticles in PBS buffer (pH 7.4) with or without 20% serum, and evidenced an
480 increase in particle size in the presence of serum, which could be due to the adsorption of
481 serum proteins to the particle surface (Narayanan et al., 2014).

482 SGF and SIF are mimicking media containing enzymes and surfactants with a determined
483 pH, 1.2 for SGF and 6.8 for SIF. In SGF and SIF, liposomes co-encapsulating SLB and DOX
484 were able to retain at least 80% of the encapsulated drugs and did not change in size during
485 12 hours (Li et al., 2018). Freeze-dried PLGA-nanoparticles co-encapsulating TMX and QUE
486 were stable in term of size, PDI and encapsulation 2 hours in SGF and 6 hours in SIF (Jain
487 et al., 2013). These results suggest good stability in the digestive tract of these nanocarriers
488 intended for oral administration.

489 3.2 *In vitro* release

490 The main goal of co-encapsulation is to deliver an optimized ratio of the two co-encapsulated
491 drugs directly to the tumor site. After defining a drug ratio leading to a positive synergistic
492 anticarcinogenic effect (positive synergistic drug ratio), similar release kinetic of the two
493 drugs from the nanocarriers allows the conservation of this defined drug ratio in the tumor
494 site.

495 To investigate whether the positive synergistic drug ratio was preserved during drug release
496 from the nanocarriers, *in vitro* release experiments were mostly performed for formulations in
497 different buffers with or without serum addition (Table 4). All *in vitro* release assays were
498 performed using the dialysis method at 37°C, except for two that used the sample and
499 separate method (Narayanan et al., 2014; Hu et al., 2016). Briefly, samples of the studied
500 nanocarriers were transferred into dialysis bags (cut off 3000 Da (Wang et al., 2019), 3500
501 Da (Fang et al., 2018; Lv et al., 2016; Mendes et al., 2014; Ramasamy et al., 2017; Wong
502 and Chiu, 2010), between 8000-14000 Da (Fatma et al., 2016; Jain et al., 2013; Li et al.,
503 2017, 2018; Ochi et al., 2016; Yu et al., 2020) or unspecified (Meng et al., 2016; Zhu et al.,
504 2017; Ray et al., 2017; Dong et al., 2017)) which were immersed in an adequate release
505 medium. For pH-sensitive nanocarriers, the release medium was adapted to study the effect
506 of pH using mainly a comparison between PBS pH 7.4 *versus* acetate buffer saline pH 5.5

507 (Ramasamy et al., 2017), phosphate-citric acidic buffered saline pH 5.5 (Dong et al., 2017) or
 508 an unspecified acidic environment (Murugan et al., 2016; Ray et al., 2017; Li et al., 2017;
 509 Fang et al., 2018; Li et al., 2018; Yu et al., 2020). For reduction-sensitive micelles, the effect
 510 of GHS concentration (reduction of a disulfide bond) on BAI and CUR release was studied by
 511 using a medium with GHS concentrations ranging from 0 to 10M in PBS (Wang et al., 2019).

512 Most release media contained surfactants (tween 80) to solubilize the lipophilic flavonoid and
 513 maintain sink conditions (Fang et al., 2018; Jain et al., 2013; Li et al., 2018; Lv et al., 2016;
 514 Mendes et al., 2014; Meng et al., 2016; Wang et al., 2015).

515 Table 4 reports the conditions of the *in vitro* release assays performed and their results. Drug
 516 release was presented as the percentage of released drug relative to the initial amount in the
 517 nanocarriers. Thus, the drug ratio could be considered as maintained when the release
 518 curves of each drug were superimposed.

519 Table 4. *In vitro* release profile of nanocarriers co-encapsulating a flavonoid with an
 520 anti-cancer agent.

In vitro release study in aqueous buffer				
Flavonoid / co-encapsulated drug	Conditions	Release of flavonoid (%) / release of other drug (%)	Ratio maintained	References
<i>Micelles</i>				
BAI/CUR	37°C PBS pH 7.4	Biphasic		(Wang et al., 2019)
	100 rpm 72 hours	0M GHS : ~30/~30	Yes	
QUE/DOX	0.5% Tween 80	1 M GHS: ~50/~60	Yes	(Ramasamy et al., 2017)
	From 0 to 10 M GSH	10 M GHS: ~80/~70	Yes	
	37°C	Biphasic		
	PBS pH 7.4			
SIL/DTX	24 hours	~7/~40	No	(Dong et al., 2017)
	72 hours	~10/~40	No	
	ABS pH 5.5			
	24 hours	~20/~68	No	
	72 hours	~25/~90	No	
	37°C 48 hours	Biphasic		
PBS 0.1 M pH 7.4		21.4/23.2	Yes	(Dong et al., 2017)
	Phosphate-citric acid buffered saline pH 5.5	79.7/82.3	Yes	
<i>Nanoemulsions</i>				
BCL/PTX	37°C PBS pH 7.4	Biphasic		(Meng et al., 2016)
	2 hours	~40/~40	Yes	
	24 hours	83.8/81.2	Yes	
0.5% (w/v) Tween-80				
<i>Solid lipid nanoparticles</i>				
BAI/DTX	37°C PBS 100 rpm			(Li et al., 2017)
	pH 7.4			
	24 hours	~70/~70	Yes	
	48 hours	~85/~85	Yes	
pH 5.0				(Li et al., 2017)
	24 hours	~85/~85	Yes	
48 hours	~85/~85	Yes		
<i>Liposomes</i>				
QUE/VIN	37°C 0.9% w/w sodium chloride		Yes	(Wong and Chiu, 2011, 2010)
	72 hours			
SIL/GCA	-37°C PBS pH 7.4 100 rpm			(Ochi et al., 2016)
SLB/DOX-HCL	48 hours	~14/~88	No	(Li et al., 2018)
	37°C 12 hours			
	3% v/v SDS			
	PBS pH 7.4	~50/~20	No	
PBS pH 2.0	~20/~70	No		

<i>Lipid-polymeric hybrid nanoparticles</i>				
QUE/VIN	37°C PBS pH 7.4 100 rpm 6 days			(Zhu et al., 2017)
GEN/PTX	37°C 125 rpm 2% SLS 48 hours 60 days	~80-90/~80-90 ~80/~10 ~80/~70	Yes No No	(Mendes et al., 2014)
<i>Polymeric nanoparticles</i>				
QUE/CUR/ASP	37°C PBS 240h pH 7.4 24 hours 7 days	Biphasic ~20/~50/~60 ~92/~85/~99	No	(Ray et al., 2017)
QUE/TMX	pH 6.5 24 hours 37°C PBS pH 7.4 2.5 w/v Tween 80 24 hours 20 days	Biphasic 44.23/24.92 94.23/85.88	No	(Jain et al., 2013)
QUE/DOX	37°C PBS pH 7.4 120 rpm 0.5% Tween 80 12 hours 240 hours	Biphasic Similar release ~25/24.12 ~90/87.34	No Yes Yes	(Lv et al., 2016)
QUE/ETO	37°C 100 rpm 0,1N HCl PBS pH 6.8 24 hours 48 hours	65.8 ± 3.4/~58 Not specified/65.6 ± 2.1	No No	(Fatma et al., 2016)
ICA/DOX	37°C PBS 1% BSA 24 hours pH 7.4 pH 5.5	35/35 >80/>80	Yes Yes	(Yu et al., 2020)
EGCG/PTX	37°C PBS pH 7.4 50 rpm 72 hours 10 days	Sequential ~49/~26 ~60/~28	No No	(Narayanan et al., 2014)
<i>Mesoporous silica nanoparticles</i>				
QUE/DOX	37°C PBS 100 rpm 1% Tween 80 pH 7.4 pH 5.0	~30/~30 ~80/~80	Yes Yes	(Fang et al., 2018)
QUE/TPT	37°C 48 hours pH 7.4 pH 6.0 pH 5.0	12.03/8.7 54.77/46.98 80.72/76.24	Yes Yes Yes	(Murugan et al., 2016)
In vitro release study in buffer supplemented with serum				
Flavonoid / co-encapsulated drug	Conditions	Release of flavonoid (%) / release of other drug (%)	Ratio maintained	References
<i>Liposomes</i>				
QUE/TMZ	37°C 10% human plasma (v/v) in PBS 12 hours 24 hours	~90/~75 ~90/~90	No	(Hu et al., 2016)
<i>Polymeric nanoparticles</i>				
EGCG/PTX	37°C PBS pH 7.4 20% serum 72 hours	~53/~25	No	(Narayanan et al., 2014)

521 ABS = acetate buffer saline, ASP = aspirin, BAI = baicalin, BCL = baicalein, CUR = curcumin, DOX = doxorubicin base,
522 DOX-HCL = doxorubicin hydrochloride, DTX = docetaxel, EGCG = (-)-Epigallocatechin gallate, ETO = etoposide, GCA =
523 glycyrrhizic acid, GEN = genistein, GHS = glutathione, HCl = hydrochloric acid, ICA = icaritin, NG = naringenin, PBS =
524 phosphate buffer saline, PMX = pemetrexed, PTX = paclitaxel, QUE = quercetin, SLB = silybin, SIL = silibinin, TMX = tamoxifen,
525 TMZ = temozolomide, TPT = topotecan, VIN = vincristine.

526 More than half of the formulations displayed a similar biphasic release kinetic of both drugs
527 from the nanocarriers and thus could maintain the original drug ratio. This could allow the
528 optimal ratio to be delivered to the tumor. However, very few teams studied the release in a
529 complex medium supplemented with serum, and when they did, the ratio was not
530 maintained. Of note, the release of EGCG and PTX from polymeric nanoparticles coated with
531 casein was the same in aqueous buffer or complex medium (Narayanan et al., 2014).

532 Co-encapsulating TMX and QUE in polymeric nanoparticles did not retain the ratio of the
533 co-encapsulated drugs during *in vitro* release or *in vivo* pharmacokinetics, suggesting that
534 the formulation needs further optimization. Even though the effect of the ratio was not
535 determined, this formulation had significantly better *in vivo* efficacy than free TMX or mixture
536 of free TMX and free QUE (Jain et al., 2013). Similarly, there was no similar release kinetic of
537 DOX and QUE from the micelles but *in vivo* experiments showed an improved efficacy of the
538 antitumor effect of the co-loaded micelles compared with the mixture of the free drugs and
539 with the DOX-loaded micelles (Ramasamy et al., 2017). In contrast, encapsulating SLB and
540 DOX-HCL in liposomes did not permit the release of both drugs according to the most
541 efficient ratio determined *in vitro* and, therefore, *in vivo* experiments did not evidence an
542 impact of the co-encapsulated SLB on the tumor growth of hepatic tumor in compared to
543 DOX-HCL encapsulated alone. However, the addition of SLB prevented cardiotoxicity. As the
544 mixture of SLB-loaded liposomes and DOX-HCL-loaded liposomes was not studied, it is
545 difficult to assess whether co-encapsulation was responsible for this effect (Li et al., 2018).
546 The initial drug ratio of SIL and GCA co-encapsulated in liposomes could not be maintained
547 during the release and no *in vivo* studies was conducted (Ochi et al., 2016).

548 In other cases, for specific applications, concomitant release was not desired but rather a
549 sequential release. Indeed, Fatma *et al* required a sequential release for optimal combined
550 efficacy, with a quicker release of QUE in order to inhibit the P-gp and enhance ETO effect
551 (Fatma et al., 2016). Similarly, Narayanan *et al* wanted to release EGCG first to sensitize
552 PTX-resistant breast tumor through glucose-regulated protein 78 inhibition (Narayanan et al.,
553 2014, 2015). When GEN and PTX were co-encapsulated in lipid-polymeric nanoparticles, a
554 temporal drug release was measured, with GEN being promptly released from the lipid
555 bilayer due to the reversibility of the phospholipid-drug interaction and PTX being released
556 when PLGA underwent degradation upon contact with water. This was of interest as GEN,
557 an antiangiogenic agent, could initiate the inhibition of neoangiogenesis while the cytotoxic
558 PTX sustainably released from the polymeric core into the tumoral tissue would promote its
559 shrinkage. The best ratio of encapsulated GEN and PTX was evaluated *in vivo* on tumor
560 growth and confirmed by of VEGF production assay and macroscopic evaluation of
561 anti-angiogenic effect (Mendes et al., 2014).

562 As mentioned earlier, few teams characterized drug release in complex medium containing
563 serum. Since flavonoids are known to bind to serum proteins (Bolli et al., 2010; Liu et al.,
564 2014), it is questionable whether the drug release would be the same as in an aqueous
565 buffer, and whether the optimized drug ratio would be maintained at the tumor site. Some
566 teams preferred to directly study the pharmacokinetics *in vivo* but did not discuss the
567 conservation of the optimized ratio, (Jain et al., 2013; Hu et al., 2016; Sandhu et al., 2017;

568 Pangen et al., 2018a; Li et al., 2018), with the exception of Wong *et al* who showed that the
569 ratio was conserved (Wong and Chiu, 2011). Narayanan *et al* evidenced *in vivo* the
570 sequential release desired (Narayanan et al., 2014).

571 3.3 Combination index

572 The main goal of combination therapy is to achieve a positive synergistic effect in order to
573 decrease the administered dose and drug-related toxicity. A combined effect that is better
574 than each drug alone does not necessarily indicates synergism, as it can be the product of
575 additivity or even a slight antagonist effect (Chou, 2010). An equation has been developed by
576 Chou and Talalay to evaluate the synergism of two drugs by the combination index (CI) from
577 cell culture experiments: $CI = (IC_{A/AB}/IC_A) + (IC_{B/AB}/IC_B)$, where IC_A and IC_B are the
578 concentrations of A or B required to kill 50% of cells when A or B are used as single agents
579 and $IC_{A/AB}$ and $IC_{B/AB}$ are the concentrations of A and B in the combination system required to
580 kill 50% of cells. Synergism is defined by $CI < 0.9$, additivity by CI between 0.9 and 1.1 and
581 antagonism by $CI > 1.1$.

582 CI was not evaluated for all nanocarriers. Studies that calculated CI are listed in Table 5. CI
583 was determined using the free drugs (Meng et al., 2016; Wong and Chiu, 2010; Wang et al.,
584 2015; Yu et al., 2020; Ramasamy et al., 2017) or the encapsulated drugs (Li et al., 2017;
585 Wang et al., 2015; Fang et al., 2018; Wong and Chiu, 2011; Zhu et al., 2017; Ray et al.,
586 2017). Evaluating the CI using free drugs can be very interesting to select a ratio before the
587 formulation step, and to apprehend which loading of each drug can be achieved. Evaluating
588 the CI using the drugs encapsulated separately or together is more accurate, because it will
589 depend on the release of each drug from the nanocarriers.

590 CI was calculated using free and encapsulated drugs in only two studies. Wong *et al*
591 reported that the best QUE:VIN ratio amongst 4 tested for synergistic effect was 1:2. They
592 confirmed this CI using single or co-encapsulated VIN and QUE. This result was expected
593 since the QUE:VIN ratio was maintained during *in vitro* release (Table 5, (Wong and Chiu,
594 2010)). Wang *et al* tested 7 BCL:PTX ratios as free or encapsulated drug. The best ratio was
595 5:1 using both conditions, and it was still the most synergistic on cells resistant to PTX
596 (Wang et al., 2015).

597 Table 5. Combination index (CI) of the flavonoids and the other anti-cancer drugs evaluated
598 for free drugs or encapsulated drugs.

Synergistic studies			
Flavonoid / co-encapsulated drug	Flavonoid:drug wt ratio with best CI (CI) study with free drugs	Flavonoid:drug wt ratio with best CI (CI) study with encapsulated drugs	References
<i>Micelles</i> QUE/DOX	4 ratios tested 1:5 (0.35, 0.58, and 0.55 in MCF-7, SCC-7, and MDA-MB-231 cancer cells respectively)		(Ramasamy et al., 2017)
<i>Nanoemulsions</i> BCL/PTX	MCF/tax cells 7 ratios tested 1:1 (0.382)		(Meng et al., 2016)
<i>Solid lipid nanoparticles</i> BAI/DTX		A549 cell line 1 ratio tested 37:63 (CI < 1)	(Li et al., 2017)
<i>Liposomes</i> QUE/VIN	4 ratios tested MDA-MB-231 cells: 1:2 (0.01) JIMT-1 cells: 1:2 (0.0000223)	1 ratio tested MDA-MB-231 cells: 1:2 (0.113) JIMT-1 cells: 1:2 (0.0900)	(Wong and Chiu, 2011, 2010)
<i>Lipid-polymer hybrid nanoparticles</i> QUE/VIN		Raji cells resistant to VIN 5 ratios tested 1:1 (0.25)	(Zhu et al., 2017)
<i>Polymeric nanoparticles</i> QUE/CUR/ASP		HCT-116 cell line Against two-drugs loaded 1 ratios but 3 dosages 2 µg/mL (0.19304) 5 µg/mL (0.33455) 10 µg/mL (0.55627)	(Ray et al., 2017)
BCL/PTX	7 ratios tested A549 cells: 5:1 (0.836) A549/PTX cells: 5:1 (0.798)	7 ratios tested A549 cells : 5:1 (0.707) A549/PTX cells :5:1 (0.513)	(Wang et al., 2015)
ICA/DOX	8 ratios tested Hepal-6 cells: 1:2 (0.24) Huh7 cells: 1:2		(Yu et al., 2020)
<i>Mesoporous silica nanoparticles</i> QUE/DOX	-	SGC7901/ADR cells 5 ratios tested 1:1 (0.19)	(Fang et al., 2018)

599 ASP = aspirin, BAI = baicalin, BCL = baicalein, CI = combination index, CUR = curcumin, DOX = doxorubicin base, DTX =
600 docetaxel, ICA = icaritin, PTX = paclitaxel, QUE = quercetin, VIN = vincristine.

601 CI is a useful index for choosing the flavonoid:anti-cancer drug ratio to be co-encapsulated.
602 However when CI was not determined, cytotoxicity assays were still performed to apprehend
603 the formulation efficacy. Various methods were used: the comparison of single and co-
604 encapsulation was evaluated (Wang et al., 2019), the co-loaded nanocarriers was compared
605 to the free drugs alone (Jain et al., 2013; Narayanan et al., 2015; Lv et al., 2016; Hu et al.,
606 2016; Murugan et al., 2016; Fatma et al., 2016; Dong et al., 2017; Li et al., 2018) or to the
607 free mixture (Jain et al., 2013; Ochi et al., 2016; Lv et al., 2016; Murugan et al., 2016; Li et
608 al., 2018). The co-encapsulating formulation could also be compared to the flavonoid
609 single-loaded nanocarrier (Narayanan et al., 2015; Hu et al., 2016) or to the anti-cancer drug
610 single loaded nanocarrier (Narayanan et al., 2015; Fatma et al., 2016; Lv et al., 2016; Dong
611 et al., 2017; Li et al., 2018). The reversal index could also be evaluated by comparing the
612 effect on cell lines resistant or not to the anti-cancer agent (Meng et al., 2016).

613 It should be noted that several other *in vitro* experiments were performed in an attempt to
614 predict the *in vivo* behavior, such as cellular uptake of the nanocarrier into tumor cells (Fatma

615 et al., 2016; Hu et al., 2016; Lv et al., 2016; Meng et al., 2016; Murugan et al., 2016; Li et al.,
616 2018; Wang et al., 2019), *in vitro* permeability assay using Caco-2 cells to assess the
617 intestinal passage (Jain et al., 2013; Sandhu et al., 2017; PANGENI et al., 2018b), effect on
618 the tumor cells protein expression (Yu et al., 2020; Fang et al., 2018; Ramasamy et al., 2017;
619 Lv et al., 2016; Narayanan et al., 2015), effect on the ROS and glutathione generation by the
620 tumor cells (Meng et al., 2016; Murugan et al., 2016; Ramasamy et al., 2017), or *in vitro*
621 migration assay to evaluate the inhibitory effect of the drug on metastasis formation (Dong et
622 al., 2017; Li et al., 2018; PANGENI et al., 2018b).

623 To conclude this section, an *in vitro* evaluation is always performed, most often to
624 demonstrate an activity (cytotoxic or otherwise) of the association and/or the co-
625 encapsulating formulation. However, there is no harmonization in the methodology used. For
626 *in vitro* release experiments, condition variations concern duration, release medium, agitation
627 and surfactant addition. It is to note the lacking of systematic MTT test and CI calculation,
628 preventing a comparison between publications results. The main interest in the future would
629 be to correlate the release ratio and the combination index to insure that a maintained
630 release ratio is directly linked to a better *in vitro* efficacy.

631 4. *In vivo* efficacy

632 Most of the nanocarriers reviewed here were investigated *in vivo* using animal model
633 experiments. It should be noted that none of these studies compared the co-loaded
634 nanocarrier to the single-loaded nanocarriers mixture. We can emphasize that even if CI or *in*
635 *vitro* release was not studied, or ratio not maintained, all formulations tested *in vivo* showed
636 efficacy.

637 4.1 Breast cancer models

638 PTX/BCL co-loaded nanoemulsions evidenced a tumor inhibition rate of 77% on MCF-7/Tax
639 tumor xenograft (Meng et al., 2016). Wong et al showed that the co-encapsulation of VIN and
640 QUE in liposomes at a synergistic ratio led to low toxicity and good antitumor efficacy in
641 estrogen negative, progesterone negative-and trastuzumab-insensitive xenograft models,
642 with a dose of VIN given at two-thirds of its maximum tolerated dose (Wong and Chiu, 2011).
643 Jain *et al*/ demonstrated that the combination of QUE and TMX in nanoparticles resulted in
644 higher antitumor efficacy on female breast tumor-bearing rats in contrast to the free drug
645 combination. In addition, co-encapsulation of an antioxidant could reduce the free radical
646 induced oxidative stress generated during the course of chronic TMX therapy (Jain et al.,
647 2013). QUE and DOX co-loaded nanoparticles significantly enhanced the *in vivo* anti-cancer
648 efficacy of DOX in a drug-resistant MCF-7/ADR xenograft model (Lv et al., 2016). Micelles
649 co-encapsulating DTX and SIL displayed a better anti-tumor effect on 4T1 tumor-bearing

650 mice compared to the free drug mixture (Dong et al., 2017). Self-emulsifying nano-emulsion
651 co-encapsulating TMX and naringenin administered orally for 30 days resulted in a lower
652 tumor burden in female breast cancer-bearing rats compared to the free drug mixture or the
653 TMX encapsulated alone. Moreover, mortality was decreased, with complete animals
654 survival for the co-encapsulating formulation (Sandhu et al., 2017). Mesoporous silica
655 nanoparticles co-encapsulating TPT and QUE showed greater tumor rate inhibition on
656 MDA-MB-231 breast tumor-bearing mice than free TPT or free QUE (Murugan et al., 2016).

657 4.2 Lung cancer models

658 Water-in-oil-in-water nanoemulsion co-encapsulating PMX and QUE for oral administration
659 improved the oral bioavailability of both drugs *in vivo* with the result of a maximum tumor
660 growth suppression in A549 cell-bearing mice (62.7%) in comparison with the control group
661 (Pangeni et al., 2018b). The pH-sensitive micelles co-encapsulating BAI and CUR had a
662 higher inhibition rate on A549 lung cancer-bearing mice than each free drugs and the single
663 encapsulated CUR (Wang et al., 2019). PLGA-nanoparticles formed by prodrugs of BCL and
664 PTX had a better effect than single-loaded nanoparticles *in vivo* on PTX-resistant A549 lung
665 tumor-bearing mice (Wang et al., 2015). Co-encapsulated DTX and BAI in solid lipid
666 nanoparticles could significantly increase the tumor inhibition rate in DTX-resistant A549
667 resistant tumor-bearing mice in comparison to single-loaded solid lipid nanoparticles, each
668 free drug or free drug mixture (Li et al., 2017). DOX and QUE co-encapsulated in micelles
669 demonstrated superior anti-cancer efficacy on SSC-7 tumor-bearing mice than free DOX,
670 free QUE, mixture of free DOX and free QUE and DOX-encapsulating micelles (Ramasamy
671 et al., 2017), even if the *in vitro* release of the drugs did not maintain the synergistic drug
672 ratio.

673 4.3 Other cancer models

674 QUE and DOX co-loaded mesoporous silica nanoparticles had a better anti-tumor effect on
675 SG7901/ADR tumor-bearing mice (gastric cancer model) than the free drugs mixture and the
676 single-loaded nanoparticles (Fang et al., 2018).

677 Cholic-acid functionalized liposomes co-encapsulating DOX-HCL and SLB displayed
678 enhanced liver accumulation and targeting, as well as more efficient inhibition of liver tumor
679 growth in H22 tumor-bearing mice and HepG2 tumor-bearing nude mice (hepatocellular
680 cancer models). In addition, co-loaded liposomes induced significantly less pathological
681 damage to the cardiac tissue compared to free DOX-HCL administered with cholic-acid
682 functionalized liposomes encapsulating only QUE (Li et al., 2018). Aminoethyl anisamide
683 functionalized nanoparticles co-encapsulating DOX and ICA showed better liver
684 accumulation, better tumor growth inhibition and better progression free survival in Hepa1-6

685 Luc tumor-bearing mice compared to DOX-nanoparticles or ICA-nanoparticles. They could
686 also remodel the immune microenvironment to suppress hepatocellular carcinoma and
687 induce better immunogenic cell death, leading to an antitumor vaccination effect (Yu et al.,
688 2020).

689 VIN and QUE co-loaded in lipid-polymeric hybrid nanoparticles showed an enhanced
690 antitumor efficacy on VIN resistant Raji tumor-bearing mice (Burkitt's lymphoma model)
691 compared to free drugs alone or in combination and to the single-loaded nanocarrier alone
692 (Zhu et al., 2017).

693 5. Concluding remarks

694 Flavonoids have been successfully co-encapsulated with anti-cancer agents in a broad range
695 of nanocarriers. As the physicochemical properties of the drugs might differ, there is a need
696 for formulation optimization depending on the drugs, and sometimes a compromise has to be
697 made (Wong and Chiu, 2011), or prodrug can be synthesized (Wang et al., 2015). If several
698 studies detailed some formulation optimization, so few reported an optimization of the
699 formulation and of the process specific to the co-encapsulation. Moreover, as the storage
700 stability of the co-encapsulating nanocarriers was rarely studied, one can wonder if those
701 nanocarriers developed are really the most suitable for the aim of co-encapsulating
702 flavonoids with an anti-cancer drug. Furthermore, the heterogeneity of the methodologies
703 used for *in vitro* experiments between these publications prevents further comparisons in
704 term of efficacy of these drug combination strategies.

705 It is also difficult to conclude on the predictive value of the combination of *in vitro* release and
706 CI. Surely, CI seems to be compulsory for selecting the best drug ratio, and *in vitro* release is
707 an almost mandatory characterization before *in vivo* experiments. However, not assessing
708 the CI or not maintaining the drug ratio during release did not prevent *in vivo* efficacy. We
709 can hypothesize that maybe the efficacy of the combination would be better at an optimized
710 drug ratio and with a similar release, but this will need confirmation (Wu et al., 2020). We can
711 also wonder if there is a more efficient way to assess the efficacy of the drug combination.
712 Recently, a study found a correlation between the Hill coefficient and the tumor response
713 after treatment by DOX co-encapsulated with either irinotecan or gemcitabine in liposomes
714 (Wu et al., 2020). Associating *in vitro* release with CI gives at least a solid clue for the *in vivo*
715 efficacy.

716 Co-encapsulation has consistently led to a better *in vivo* anti-tumor effect compared to free
717 drugs, a mixture of free drugs or one drug encapsulated alone into the nanocarriers. As
718 co-encapsulation can be challenging, it is questionable whether co-encapsulation is worth
719 the effort. For example, Mura *et al* evidenced that co-encapsulating sunitinib and

720 gemcitabine in squalene nanoparticles was as efficient *in vitro* as the mixture of the drug
721 encapsulated alone in squalene nanoparticles, but did not confirm this result *in vivo* (Mura et
722 al., 2016). On the other hand, liposomes co-encapsulating cytarabine and daunorubicin in a
723 5:1 ratio (CPX-351) against acute myeloid leukemia was approved by the FDA and EMA
724 (Alfayez et al., 2020; Tardi et al., 2009). Moreover, Markovsky *et al* evidenced that PTX and
725 DOX conjugated to PGA nanoparticles significantly increased the tumor inhibition rate on
726 MDA-MB-231 tumor-bearing mice compared to a mixture of individually-conjugated drugs or
727 free drug combination (Markovsky et al., 2014). This leads to the idea that co-encapsulation
728 might be a promising approach. However, with regard to the co-encapsulation of flavonoids
729 with an anti-cancer agent, this review highlights the absence of mixture of the individually
730 encapsulated drugs as a control group *in vitro* or *in vivo* to be able to evidence a significant
731 advantage of the co-encapsulation.

732 Due to the pleiotropic properties of flavonoids, some groups specifically studied the
733 antioxidant (Jain et al., 2013; Li et al., 2018), antiangiogenic (Jain et al., 2013; Mendes et al.,
734 2014), anti-metastasis (Dong et al., 2017) or macrophage reprogramming (Wang et al.,
735 2019) properties of these molecules in order to evaluate their co-encapsulated formulation *in*
736 *vitro* and/or *in vivo*. Some showed a decreased in toxicity on some vital organs (Jain et al.,
737 2013; Li et al., 2018), or other an antiangiogenic effect within the tumor site (Jain et al., 2013;
738 Mendes et al., 2014). This approach should be generalized for every design of nanocarriers
739 co-encapsulating a flavonoid to highlight its additional effects.

740 7. Acknowledgments: na

741 8. Fundings: This research did not receive any specific grant from funding agencies in the
742 public, commercial, or not-for-profit sectors. M.R.M. was partially supported by le Prix de la
743 médaille (Assistance Publique – Hôpitaux de Paris) and l'Année Recherche.

744 9. References

- 745 Adan, A., Baran, Y., 2015. The pleiotropic effects of fisetin and hesperetin on human acute
746 promyelocytic leukemia cells are mediated through apoptosis, cell cycle arrest, and
747 alterations in signaling networks. *Tumour Biol.* 36, 8973–8984.
748 <https://doi.org/10.1007/s13277-015-3597-6>
- 749 Ahmad, A., Ali, T., Park, H.Y., Badshah, H., Rehman, S.U., Kim, M.O., 2016. Neuroprotective Effect of
750 Fisetin Against Amyloid-Beta-Induced Cognitive/Synaptic Dysfunction, Neuroinflammation,
751 and Neurodegeneration in Adult Mice. *Mol. Neurobiol.* <https://doi.org/10.1007/s12035-016-9795-4>
- 752
753 Aiello, P., Consalvi, S., Poce, G., Raguzzini, A., Toti, E., Palmery, M., Biava, M., Bernardi, M., Kamal,
754 M.A., Perry, G., Peluso, I., 2019. Dietary flavonoids: Nano delivery and nanoparticles for
755 cancer therapy. *Semin. Cancer Biol.* <https://doi.org/10.1016/j.semcancer.2019.08.029>

756 Akbarzadeh, A., Rezaei-Sadabady, R., Davaran, S., Joo, S.W., Zarghami, N., Hanifehpour, Y., Samiei,
757 M., Kouhi, M., Nejati-Koshki, K., 2013. Liposome: classification, preparation, and applications.
758 *Nanoscale Res Lett* 8, 102. <https://doi.org/10.1186/1556-276X-8-102>
759 Alfayez, M., Kantarjian, H., Kadia, T., Ravandi-Kashani, F., Daver, N., 2020. CPX-351 (vyxeos) in AML.
760 *Leuk. Lymphoma* 61, 288–297. <https://doi.org/10.1080/10428194.2019.1660970>
761 Bayat Mokhtari, R., Homayouni, T.S., Baluch, N., Morgatskaya, E., Kumar, S., Das, B., Yeger, H., 2017.
762 Combination therapy in combating cancer. *Oncotarget* 8, 38022–38043.
763 <https://doi.org/10.18632/oncotarget.16723>
764 Bednarek, P., Kerhoas, L., Einhorn, J., Frański, R., Wojtaszek, P., Rybus-Zajac, M., Stobiecki, M., 2003.
765 Profiling of Flavonoid Conjugates in *Lupinus albus* and *Lupinus angustifolius* Responding to
766 Biotic and Abiotic Stimuli. *J Chem Ecol* 29, 1127–1142.
767 <https://doi.org/10.1023/A:1023877422403>
768 Bensikaddour, H., Fa, N., Burton, I., Deleu, M., Lins, L., Schanck, A., Brasseur, R., Dufrêne, Y.F.,
769 Goormaghtigh, E., Mingeot-Leclercq, M.-P., 2008. Characterization of the Interactions
770 between Fluoroquinolone Antibiotics and Lipids: a Multitechnique Approach. *Biophys J* 94,
771 3035–3046. <https://doi.org/10.1529/biophysj.107.114843>
772 Bolli, A., Marino, M., Rimbach, G., Fanali, G., Fasano, M., Ascenzi, P., 2010. Flavonoid binding to
773 human serum albumin. *Biochemical and Biophysical Research Communications* 398, 444–
774 449. <https://doi.org/10.1016/j.bbrc.2010.06.096>
775 Carvalho, D., Paulino, M., Polticelli, F., Arredondo, F., Williams, R.J., Abin-Carriquiry, J.A., 2017.
776 Structural evidence of quercetin multi-target bioactivity: A reverse virtual screening strategy.
777 *Eur J Pharm Sci* 106, 393–403. <https://doi.org/10.1016/j.ejps.2017.06.028>
778 Chaaban, H., Ioannou, I., Chebil, L., Slimane, M., Gérardin, C., Paris, C., Charbonnel, C., Chekir, L.,
779 Ghoum, M., 2017. Effect of heat processing on thermal stability and antioxidant activity of six
780 flavonoids. *Journal of Food Processing and Preservation* 41, e13203.
781 <https://doi.org/10.1111/jfpp.13203>
782 Chen, Chengjun, Han, D., Cai, C., Tang, X., 2010. An overview of liposome lyophilization and its future
783 potential. *Journal of Controlled Release* 142, 299–311.
784 <https://doi.org/10.1016/j.jconrel.2009.10.024>
785 Chen, Chen, Zhou, J., Ji, C., 2010. Quercetin: a potential drug to reverse multidrug resistance. *Life Sci.*
786 87, 333–338. <https://doi.org/10.1016/j.lfs.2010.07.004>
787 Chen, J., Lin, H., Hu, M., 2003. Metabolism of Flavonoids via Enteric Recycling: Role of Intestinal
788 Disposition. *J Pharmacol Exp Ther* 304, 1228–1235. <https://doi.org/10.1124/jpet.102.046409>
789 Choi, H.S., Liu, W., Misra, P., Tanaka, E., Zimmer, J.P., Ipe, B.I., Bawendi, M.G., Frangioni, J.V., 2007.
790 Renal Clearance of Nanoparticles. *Nat Biotechnol* 25, 1165–1170.
791 <https://doi.org/10.1038/nbt1340>
792 Choi, J.Y., Thapa, R.K., Yong, C.S., Kim, J.O., 2016. Nanoparticle-based combination drug delivery
793 systems for synergistic cancer treatment. *Journal of Pharmaceutical Investigation* 46, 325–
794 339. <https://doi.org/10.1007/s40005-016-0252-1>
795 Chou, T.-C., 2010. Drug combination studies and their synergy quantification using the Chou-Talalay
796 method. *Cancer Res.* 70, 440–446. <https://doi.org/10.1158/0008-5472.CAN-09-1947>
797 Corradini, E., Foglia, P., Giansanti, P., Gubbio, R., Samperi, R., Lagana, A., 2011. Flavonoids:
798 chemical properties and analytical methodologies of identification and quantitation in foods
799 and plants. *Nat. Prod. Res.* 25, 469–495. <https://doi.org/10.1080/14786419.2010.482054>
800 Cosco, D., Paolino, D., Maiuolo, J., Russo, D., Fresta, M., 2011. Liposomes as multicompartmental
801 carriers for multidrug delivery in anticancer chemotherapy. *Drug Deliv. and Transl. Res.* 1,
802 66–75. <https://doi.org/10.1007/s13346-010-0007-x>
803 Crozier, A., Del Rio, D., Clifford, M.N., 2010. Bioavailability of dietary flavonoids and phenolic
804 compounds. *Mol. Aspects Med.* 31, 446–467. <https://doi.org/10.1016/j.mam.2010.09.007>
805 Cui, J., Liu, X., Chow, L.M.C., 2019. Flavonoids as P-gp Inhibitors: A Systematic Review of SARs. *Curr.*
806 *Med. Chem.* 26, 4799–4831. <https://doi.org/10.2174/0929867325666181001115225>

807 Dayoub, O., Andriantsitohaina, R., Clere, N., 2013. Pleiotropic beneficial effects of epigallocatechin
808 gallate, quercetin and delphinidin on cardiovascular diseases associated with endothelial
809 dysfunction. *Cardiovasc Hematol Agents Med Chem* 11, 249–264.
810 <https://doi.org/10.2174/1871525712666140309233048>

811 Dong, X.-Y., Lang, T.-Q., Yin, Q., Zhang, P.-C., Li, Y.-P., 2017. Co-delivery of docetaxel and silibinin
812 using pH-sensitive micelles improves therapy of metastatic breast cancer. *Acta Pharmacol.*
813 *Sin.* 38, 1655–1662. <https://doi.org/10.1038/aps.2017.74>

814 Fang, J., Zhang, S., Xue, X., Zhu, X., Song, S., Wang, B., Jiang, L., Qin, M., Liang, H., Gao, L., 2018.
815 Quercetin and doxorubicin co-delivery using mesoporous silica nanoparticles enhance the
816 efficacy of gastric carcinoma chemotherapy. *Int J Nanomedicine* 13, 5113–5126.
817 <https://doi.org/10.2147/IJN.S170862>

818 Fatma, S., Talegaonkar, S., Iqbal, Z., Panda, A.K., Negi, L.M., Goswami, D.G., Tariq, M., 2016. Novel
819 flavonoid-based biodegradable nanoparticles for effective oral delivery of etoposide by P-
820 glycoprotein modulation: an in vitro, ex vivo and in vivo investigations. *Drug Deliv* 23, 500–
821 511. <https://doi.org/10.3109/10717544.2014.923956>

822 Gaber, D.M., Nafee, N., Abdallah, O.Y., 2017. Myricetin solid lipid nanoparticles: Stability assurance
823 from system preparation to site of action. *European Journal of Pharmaceutical Sciences* 109,
824 569–580. <https://doi.org/10.1016/j.ejps.2017.08.007>

825 Gao, W., Ye, G., Duan, X., Yang, X., Yang, V.C., 2017. Transferrin receptor-targeted pH-sensitive
826 micellar system for diminution of drug resistance and targetable delivery in multidrug-
827 resistant breast cancer. *Int J Nanomedicine* 12, 1047–1064.
828 <https://doi.org/10.2147/IJN.S115215>

829 Gaumet, M., Vargas, A., Gurny, R., Delie, F., 2008. Nanoparticles for drug delivery: The need for
830 precision in reporting particle size parameters. *European Journal of Pharmaceutics and*
831 *Biopharmaceutics* 69, 1–9. <https://doi.org/10.1016/j.ejpb.2007.08.001>

832 Gupta, S.C., Kunnumakkara, A.B., Aggarwal, S., Aggarwal, B.B., 2018. Inflammation, a Double-Edge
833 Sword for Cancer and Other Age-Related Diseases. *Front Immunol* 9, 2160.
834 <https://doi.org/10.3389/fimmu.2018.02160>

835 Gurunathan, S., Kang, M.-H., Qasim, M., Kim, J.-H., 2018. Nanoparticle-Mediated Combination
836 Therapy: Two-in-One Approach for Cancer. *Int J Mol Sci* 19.
837 <https://doi.org/10.3390/ijms19103264>

838 Hadinoto, K., Sundaresan, A., Cheow, W.S., 2013. Lipid–polymer hybrid nanoparticles as a new
839 generation therapeutic delivery platform: A review. *European Journal of Pharmaceutics and*
840 *Biopharmaceutics* 85, 427–443. <https://doi.org/10.1016/j.ejpb.2013.07.002>

841 Harasym, T.O., Tardi, P.G., Harasym, N.L., Harvie, P., Johnstone, S.A., Mayer, L.D., 2007. Increased
842 preclinical efficacy of irinotecan and floxuridine coencapsulated inside liposomes is
843 associated with tumor delivery of synergistic drug ratios. *Oncol. Res.* 16, 361–374.
844 <https://doi.org/10.3727/000000006783980937>

845 He, X.-G., 2000. On-line identification of phytochemical constituents in botanical extracts by
846 combined high-performance liquid chromatographic–diode array detection–mass
847 spectrometric techniques. *Journal of Chromatography A* 880, 203–232.
848 [https://doi.org/10.1016/S0021-9673\(00\)00059-5](https://doi.org/10.1016/S0021-9673(00)00059-5)

849 Hinderer, W., Seitz, H.U., 1988. CHAPTER 2 - Flavonoids, in: Constabel, F., Vasil, I.K. (Eds.),
850 *Phytochemicals in Plant Cell Cultures*. Academic Press, pp. 23–48.
851 <https://doi.org/10.1016/B978-0-12-715005-5.50009-1>

852 Hu, C.-M.J., Aryal, S., Zhang, L., 2010. Nanoparticle-assisted combination therapies for effective
853 cancer treatment. *Ther Deliv* 1, 323–334. <https://doi.org/10.4155/tde.10.13>

854 Hu, J., Wang, J., Wang, G., Yao, Z., Dang, X., 2016. Pharmacokinetics and antitumor efficacy of DSPE-
855 PEG2000 polymeric liposomes loaded with quercetin and temozolomide: Analysis of their
856 effectiveness in enhancing the chemosensitization of drug-resistant glioma cells. *Int J Mol*
857 *Med* 37, 690–702. <https://doi.org/10.3892/ijmm.2016.2458>

858 Jackman, R.L., Yada, R.Y., Tung, M.A., Speers, R.A., 1987. Anthocyanins as Food Colorants —a Review.
859 Journal of Food Biochemistry 11, 201–247. <https://doi.org/10.1111/j.1745->
860 4514.1987.tb00123.x

861 Jain, A.K., Thanki, K., Jain, S., 2013. Co-encapsulation of Tamoxifen and Quercetin in Polymeric
862 Nanoparticles: Implications on Oral Bioavailability, Antitumor Efficacy, and Drug-Induced
863 Toxicity. Mol. Pharmaceutics 10, 3459–3474. <https://doi.org/10.1021/mp400311j>

864 Je, L., Gl, U., Je, C., Lf, N., Tl, L., Ek, R., Rk, S., Sa, S., D, H., Sr, S., Rm, S., Dl, B., Je, K., Gj, S., Mj, W., Dh,
865 R., A, H., K, B., M, C., Ac, L., Bc, M., 2018. CPX-351 (cytarabine and daunorubicin) Liposome
866 for Injection Versus Conventional Cytarabine Plus Daunorubicin in Older Patients With Newly
867 Diagnosed Secondary Acute Myeloid Leukemia. Journal of clinical oncology : official journal
868 of the American Society of Clinical Oncology 36. <https://doi.org/10.1200/JCO.2017.77.6112>

869 Kashyap, D., Garg, V.K., Tuli, H.S., Yerer, M.B., Sak, K., Sharma, A.K., Kumar, M., Aggarwal, V., Sandhu,
870 S.S., 2019. Fisetin and Quercetin: Promising Flavonoids with Chemopreventive Potential.
871 Biomolecules 9, 174. <https://doi.org/10.3390/biom9050174>

872 Khushnud, T., Mousa, S.A., 2013. Potential Role of Naturally Derived Polyphenols and Their
873 Nanotechnology Delivery in Cancer. Mol Biotechnol 55, 78–86.
874 <https://doi.org/10.1007/s12033-012-9623-7>

875 Kikuchi, H., Yuan, B., Hu, X., Okazaki, M., 2019. Chemopreventive and anticancer activity of flavonoids
876 and its possibility for clinical use by combining with conventional chemotherapeutic agents.
877 Am J Cancer Res 9, 1517–1535.

878 Kumar, S., Pandey, A.K., 2013. Chemistry and biological activities of flavonoids: an overview.
879 ScientificWorldJournal 2013, 162750. <https://doi.org/10.1155/2013/162750>

880 Lee, R.-S., Lin, C.-H., Aljuffali, I.A., Hu, K.-Y., Fang, J.-Y., 2015. Passive targeting of thermosensitive
881 diblock copolymer micelles to the lungs: synthesis and characterization of poly(N-
882 isopropylacrylamide)-block-poly(ϵ -caprolactone). J Nanobiotechnology 13.
883 <https://doi.org/10.1186/s12951-015-0103-7>

884 Li, S., Wang, L., Li, N., Liu, Y., Su, H., 2017. Combination lung cancer chemotherapy: Design of a pH-
885 sensitive transferrin-PEG-Hz-lipid conjugate for the co-delivery of docetaxel and baicalin.
886 Biomedicine & Pharmacotherapy 95, 548–555. <https://doi.org/10.1016/j.biopha.2017.08.090>

887 Li, Y., Yang, D., Wang, Y., Li, Z., Zhu, C., 2018. Co-delivery doxorubicin and silybin for anti-hepatoma
888 via enhanced oral hepatic-targeted efficiency. Int J Nanomedicine 14, 301–315.
889 <https://doi.org/10.2147/IJN.S187888>

890 Liu, S., Guo, C., Guo, Y., Yu, H., Greenaway, F., Sun, M.-Z., 2014. Comparative Binding Affinities of
891 Flavonoid Phytochemicals with Bovine Serum Albumin. Iran J Pharm Res 13, 1019–1028.

892 Lv, L., Liu, C., Chen, C., Yu, X., Chen, G., Shi, Y., Qin, F., Ou, J., Qiu, K., Li, G., 2016. Quercetin and
893 doxorubicin co-encapsulated biotin receptor-targeting nanoparticles for minimizing drug
894 resistance in breast cancer. Oncotarget 7, 32184–32199.
895 <https://doi.org/10.18632/oncotarget.8607>

896 Markovsky, E., Baabur-Cohen, H., Satchi-Fainaro, R., 2014. Anticancer polymeric nanomedicine
897 bearing synergistic drug combination is superior to a mixture of individually-conjugated
898 drugs. Journal of Controlled Release 187, 145–157.
899 <https://doi.org/10.1016/j.jconrel.2014.05.025>

900 Mayer, L.D., Harasym, T.O., Tardi, P.G., Harasym, N.L., Shew, C.R., Johnstone, S.A., Ramsay, E.C.,
901 Bally, M.B., Janoff, A.S., 2006. Ratiometric dosing of anticancer drug combinations:
902 Controlling drug ratios after systemic administration regulates therapeutic activity in tumor-
903 bearing mice. Mol Cancer Ther 5, 1854–1863. <https://doi.org/10.1158/1535-7163.MCT-06->
904 0118

905 Mehnert, W., Mäder, K., 2001. Solid lipid nanoparticles: Production, characterization and
906 applications. Advanced Drug Delivery Reviews, Lipid Assemblies for Drug Delivery 47, 165–
907 196. [https://doi.org/10.1016/S0169-409X\(01\)00105-3](https://doi.org/10.1016/S0169-409X(01)00105-3)

908 Mendes, L.P., Gaeti, M.P.N., Ávila, P.H.M. de, Vieira, M. de S., Rodrigues, B. dos S., Marcelino, R.I. de
909 Á., Santos, L.C.R. dos, Valadares, M.C., Lima, E.M., 2014. Multicompartmental Nanoparticles

910 for Co-Encapsulation and Multimodal Drug Delivery to Tumor Cells and Neovasculature.
911 Pharm Res 31, 1106–1119. <https://doi.org/10.1007/s11095-013-1234-x>

912 Meng, L., Xia, X., Yang, Y., Ye, J., Dong, W., Ma, P., Jin, Y., Liu, Y., 2016. Co-encapsulation of paclitaxel
913 and baicalein in nanoemulsions to overcome multidrug resistance via oxidative stress
914 augmentation and P-glycoprotein inhibition. *International Journal of Pharmaceutics* 513, 8–
915 16. <https://doi.org/10.1016/j.ijpharm.2016.09.001>

916 Mignet, N., Seguin, J., Chabot, G.G., 2013. Bioavailability of Polyphenol Liposomes: A Challenge
917 Ahead. *Pharmaceutics* 5, 457–471. <https://doi.org/10.3390/pharmaceutics5030457>

918 Mingeot-Leclercq, M.-P., Gallet, X., Flore, C., Van Bambeke, F., Peuvot, J., Brasseur, R., 2001.
919 Experimental and Conformational Analyses of Interactions between Butenafine and Lipids.
920 *Antimicrob Agents Chemother* 45, 3347–3354. [https://doi.org/10.1128/AAC.45.12.3347-](https://doi.org/10.1128/AAC.45.12.3347-3354.2001)
921 [3354.2001](https://doi.org/10.1128/AAC.45.12.3347-3354.2001)

922 Mirossay, L., Varinská, L., Mojžiš, J., 2017. Antiangiogenic Effect of Flavonoids and Chalcones: An
923 Update. *Int J Mol Sci* 19. <https://doi.org/10.3390/ijms19010027>

924 Moghimi, S.M., Hunter, A.C., Murray, J.C., 2001. Long-circulating and target-specific nanoparticles:
925 theory to practice. *Pharmacological reviews* 53, 283–318.

926 Mohapatra, M., Mishra, A.K., 2011. Photophysical Behavior of Fisetin in
927 Dimyristoylphosphatidylcholine Liposome Membrane. *The Journal of Physical Chemistry B*
928 115, 9962–9970. <https://doi.org/10.1021/jp1123212>

929 Mura, S., Buchy, E., Askin, G., Cayre, F., Mougín, J., Gouazou, S., Sobot, D., Valetti, S., Stella, B.,
930 Desmaele, D., Couvreur, P., 2016. In vitro investigation of multidrug nanoparticles for
931 combined therapy with gemcitabine and a tyrosine kinase inhibitor: Together is not better.
932 *Biochimie, Lipidomics and Functional Lipid Biology* 130, 4–13.
933 <https://doi.org/10.1016/j.biochi.2016.08.003>

934 Murugan, C., Rayappan, K., Thangam, R., Bhanumathi, R., Shanthy, K., Vivek, R., Thirumurugan, R.,
935 Bhattacharyya, A., Sivasubramanian, S., Gunasekaran, P., Kannan, S., 2016. Combinatorial
936 nanocarrier based drug delivery approach for amalgamation of anti-tumor agents in breast
937 cancer cells: an improved nanomedicine strategies. *Sci Rep* 6.
938 <https://doi.org/10.1038/srep34053>

939 Nagaraju, G.P., Zafar, S.F., El-Rayes, B.F., 2013. Pleiotropic effects of genistein in metabolic,
940 inflammatory, and malignant diseases. *Nutr. Rev.* 71, 562–572.
941 <https://doi.org/10.1111/nure.12044>

942 Narayan, R., Nayak, U.Y., Raichur, A.M., Garg, S., 2018. Mesoporous Silica Nanoparticles: A
943 Comprehensive Review on Synthesis and Recent Advances. *Pharmaceutics* 10.
944 <https://doi.org/10.3390/pharmaceutics10030118>

945 Narayanan, S., Mony, U., Vijaykumar, D.K., Koyakutty, M., Paul-Prasanth, B., Menon, D., 2015.
946 Sequential release of epigallocatechin gallate and paclitaxel from PLGA-casein core/shell
947 nanoparticles sensitizes drug-resistant breast cancer cells. *Nanomedicine* 11, 1399–1406.
948 <https://doi.org/10.1016/j.nano.2015.03.015>

949 Narayanan, S., Pavithran, M., Viswanath, A., Narayanan, D., Mohan, C.C., Manzoor, K., Menon, D.,
950 2014. Sequentially releasing dual-drug-loaded PLGA–casein core/shell nanomedicine: Design,
951 synthesis, biocompatibility and pharmacokinetics. *Acta Biomaterialia* 10, 2112–2124.
952 <https://doi.org/10.1016/j.actbio.2013.12.041>

953 Ochi, M.M., Amoabediny, G., Rezayat, S.M., Akbarzadeh, A., Ebrahimi, B., 2016. In Vitro Co-Delivery
954 Evaluation of Novel Pegylated Nano-Liposomal Herbal Drugs of Silibinin and Glycyrrhizic Acid
955 (Nano-Phytosome) to Hepatocellular Carcinoma Cells. *Cell J* 18, 135–148.
956 <https://doi.org/10.22074/cellj.2016.4308>

957 Pan, J., Rostamizadeh, K., Filipczak, N., Torchilin, V.P., 2019. Polymeric Co-Delivery Systems in Cancer
958 Treatment: An Overview on Component Drugs' Dosage Ratio Effect. *Molecules* 24.
959 <https://doi.org/10.3390/molecules24061035>

960 Panche, A.N., Diwan, A.D., Chandra, S.R., 2016. Flavonoids: an overview. *J Nutr Sci* 5.
961 <https://doi.org/10.1017/jns.2016.41>

962 Pangeni, R., Choi, J.U., Panthi, V.K., Byun, Y., Park, J.W., 2018a. Enhanced oral absorption of
963 pemetrexed by ion-pairing complex formation with deoxycholic acid derivative and multiple
964 nanoemulsion formulations: preparation, characterization, and in vivo oral bioavailability and
965 anticancer effect. *Int J Nanomedicine* 13, 3329–3351. <https://doi.org/10.2147/IJN.S167958>
966 Pangeni, R., Choi, S.W., Jeon, O.-C., Byun, Y., Park, J.W., 2016. Multiple nanoemulsion system for an
967 oral combinational delivery of oxaliplatin and 5-fluorouracil: preparation and in vivo
968 evaluation. *Int J Nanomedicine* 11, 6379–6399. <https://doi.org/10.2147/IJN.S121114>
969 Pangeni, R., Panthi, V.K., Yoon, I.-S., Park, J.W., 2018b. Preparation, Characterization, and In Vivo
970 Evaluation of an Oral Multiple Nanoemulsive System for Co-Delivery of Pemetrexed and
971 Quercetin. *Pharmaceutics* 10. <https://doi.org/10.3390/pharmaceutics10030158>
972 Peer, D., Karp, J.M., Hong, S., Farokhzad, O.C., Margalit, R., Langer, R., 2007. Nanocarriers as an
973 emerging platform for cancer therapy. *Nature Nanotech* 2, 751–760.
974 <https://doi.org/10.1038/nnano.2007.387>
975 Plaza, M., Pozzo, T., Liu, J., Gulshan Ara, K.Z., Turner, C., Nordberg Karlsson, E., 2014. Substituent
976 Effects on in Vitro Antioxidizing Properties, Stability, and Solubility in Flavonoids. *J. Agric.*
977 *Food Chem.* 62, 3321–3333. <https://doi.org/10.1021/jf405570u>
978 Ramasamy, T., Ruttala, H.B., Chitrapriya, N., Poudal, B.K., Choi, J.Y., Kim, S.T., Youn, Y.S., Ku, S.K.,
979 Choi, H.-G., Yong, C.S., Kim, J.O., 2017. Engineering of cell microenvironment-responsive
980 polypeptide nanovehicle co-encapsulating a synergistic combination of small molecules for
981 effective chemotherapy in solid tumors. *Acta Biomaterialia* 48, 131–143.
982 <https://doi.org/10.1016/j.actbio.2016.10.034>
983 Ramešová, Š., Sokolová, R., Degano, I., 2015. The study of the oxidation of the natural flavonol fisetin
984 confirmed quercetin oxidation mechanism. *Electrochimica Acta* 182, 544–549.
985 <https://doi.org/10.1016/j.electacta.2015.09.144>
986 Ray, L., Pal, M.K., Ray, R.S., 2017. Synergism of co-delivered nanosized antioxidants displayed
987 enhanced anticancer efficacy in human colon cancer cell lines. *Bioactive Materials* 2, 82–95.
988 <https://doi.org/10.1016/j.bioactmat.2017.02.003>
989 Reyes-Farias, M., Carrasco-Pozo, C., 2019. The Anti-Cancer Effect of Quercetin: Molecular
990 Implications in Cancer Metabolism. *Int J Mol Sci* 20. <https://doi.org/10.3390/ijms20133177>
991 Samie, A., Sedaghat, R., Baluchnejadmojarad, T., Roghani, M., 2018. Hesperetin, a citrus flavonoid,
992 attenuates testicular damage in diabetic rats via inhibition of oxidative stress, inflammation,
993 and apoptosis. *Life Sci.* 210, 132–139. <https://doi.org/10.1016/j.lfs.2018.08.074>
994 Sandhu, P.S., Kumar, R., Beg, S., Jain, S., Kushwah, V., Katare, O.P., Singh, B., 2017. Natural lipids
995 enriched self-nano-emulsifying systems for effective co-delivery of tamoxifen and naringenin:
996 Systematic approach for improved breast cancer therapeutics. *Nanomedicine* 13, 1703–
997 1713. <https://doi.org/10.1016/j.nano.2017.03.003>
998 Savić, R., Eisenberg, A., Maysinger, D., 2006. Block copolymer micelles as delivery vehicles of
999 hydrophobic drugs: Micelle–cell interactions. *Journal of Drug Targeting* 14, 343–355.
1000 <https://doi.org/10.1080/10611860600874538>
1001 Seguin, J., Brullé, L., Boyer, R., Lu, Y.M., Ramos Romano, M., Touil, Y.S., Scherman, D., Bessodes, M.,
1002 Mignet, N., Chabot, G.G., 2013. Liposomal encapsulation of the natural flavonoid fisetin
1003 improves bioavailability and antitumor efficacy. *Int J Pharm* 444, 146–154.
1004 <https://doi.org/10.1016/j.ijpharm.2013.01.050>
1005 Smith, G.J., Thomsen, S.J., Markham, K.R., Andary, C., Cardon, D., 2000. The photostabilities of
1006 naturally occurring 5-hydroxyflavones, flavonols, their glycosides and their aluminium
1007 complexes. *Journal of Photochemistry and Photobiology A: Chemistry* 136, 87–91.
1008 [https://doi.org/10.1016/S1010-6030\(00\)00320-8](https://doi.org/10.1016/S1010-6030(00)00320-8)
1009 Sokolová, R., Ramešová, Š., Degano, I., Hromadová, M., Gál, M., Žabka, J., 2012. The oxidation of
1010 natural flavonoid quercetin. *Chem. Commun.* 48, 3433–3435.
1011 <https://doi.org/10.1039/C2CC18018A>
1012 Su, S.-J., Yeh, T.-M., Chuang, W.-J., Ho, C.-L., Chang, K.-L., Cheng, Hsiao-Ling, Liu, H.-S., Cheng, Hong-
1013 Lin, Hsu, P.-Y., Chow, N.-H., 2005. The novel targets for anti-angiogenesis of genistein on

1014 human cancer cells. *Biochem. Pharmacol.* 69, 307–318.
1015 <https://doi.org/10.1016/j.bcp.2004.09.025>

1016 Tagne, J.-B., Kakumanu, S., Nicolosi, R.J., 2008. Nanoemulsion Preparations of the Anticancer Drug
1017 Dacarbazine Significantly Increase Its Efficacy in a Xenograft Mouse Melanoma Model. *Mol.*
1018 *Pharmaceutics* 5, 1055–1063. <https://doi.org/10.1021/mp8000556>

1019 Tardi, P., Johnstone, S., Harasym, N., Xie, S., Harasym, T., Zisman, N., Harvie, P., Bermudes, D., Mayer,
1020 L., 2009. In vivo maintenance of synergistic cytarabine:daunorubicin ratios greatly enhances
1021 therapeutic efficacy. *Leukemia Research* 33, 129–139.
1022 <https://doi.org/10.1016/j.leukres.2008.06.028>

1023 Tardi, P.G., Gallagher, R.C., Johnstone, S., Harasym, N., Webb, M., Bally, M.B., Mayer, L.D., 2007.
1024 Coencapsulation of irinotecan and floxuridine into low cholesterol-containing liposomes that
1025 coordinate drug release in vivo. *Biochimica et Biophysica Acta (BBA) - Biomembranes* 1768,
1026 678–687. <https://doi.org/10.1016/j.bbamem.2006.11.014>

1027 Touil, Y.S., Fellous, A., Scherman, D., Chabot, G.G., 2009. Flavonoid-Induced Morphological
1028 Modifications of Endothelial Cells Through Microtubule Stabilization. *Nutrition and Cancer*
1029 61, 310–321. <https://doi.org/10.1080/01635580802521346>

1030 Touil, Y.S., Seguin, J., Scherman, D., Chabot, G.G., 2011. Improved antiangiogenic and antitumour
1031 activity of the combination of the natural flavonoid fisetin and cyclophosphamide in Lewis
1032 lung carcinoma-bearing mice. *Cancer Chemotherapy and Pharmacology* 68, 445–455.
1033 <https://doi.org/10.1007/s00280-010-1505-8>

1034 Tsao, R., 2010. Chemistry and Biochemistry of Dietary Polyphenols. *Nutrients* 2, 1231–1246.
1035 <https://doi.org/10.3390/nu2121231>

1036 Wang, B., Zhang, W., Zhou, X., Liu, M., Hou, X., Cheng, Z., Chen, D., 2019. Development of dual-
1037 targeted nano-dandelion based on an oligomeric hyaluronic acid polymer targeting tumor-
1038 associated macrophages for combination therapy of non-small cell lung cancer. *Drug Delivery*
1039 26, 1265–1279. <https://doi.org/10.1080/10717544.2019.1693707>

1040 Wang, J., Zhao, X.-H., 2016. Degradation kinetics of fisetin and quercetin in solutions as effected by
1041 pH, temperature and coexisted proteins. *Journal of the Serbian Chemical Society* 81, 243–
1042 253. <https://doi.org/10.2298/JSC150706092W>

1043 Wang, W., Xi, M., Duan, X., Wang, Y., Kong, F., 2015. Delivery of baicalein and paclitaxel using self-
1044 assembled nanoparticles: synergistic antitumor effect in vitro and in vivo. *Int J Nanomedicine*
1045 10, 3737–3750. <https://doi.org/10.2147/IJN.S80297>

1046 Wong, M.-Y., Chiu, G.N.C., 2011. Liposome formulation of co-encapsulated vincristine and quercetin
1047 enhanced antitumor activity in a trastuzumab-insensitive breast tumor xenograft model.
1048 *Nanomedicine: Nanotechnology, Biology and Medicine* 7, 834–840.
1049 <https://doi.org/10.1016/j.nano.2011.02.001>

1050 Wong, M.-Y., Chiu, G.N.C., 2010. Simultaneous liposomal delivery of quercetin and vincristine for
1051 enhanced estrogen-receptor-negative breast cancer treatment. *Anticancer Drugs* 21, 401–
1052 410. <https://doi.org/10.1097/CAD.0b013e328336e940>

1053 Wu, D., Pusuluri, A., Vogus, D., Krishnan, V., Shields, C.W., Kim, J., Razmi, A., Mitragotri, S., 2020.
1054 Design principles of drug combinations for chemotherapy. *Journal of Controlled Release* 323,
1055 36–46. <https://doi.org/10.1016/j.jconrel.2020.04.018>

1056 Wu, L., Bi, Y., Wu, H., 2018. Formulation optimization and the absorption mechanisms of
1057 nanoemulsion in improving baicalin oral exposure. *Drug Development and Industrial*
1058 *Pharmacy* 44, 266–275. <https://doi.org/10.1080/03639045.2017.1391831>

1059 Yao, Y., Lin, G., Xie, Y., Ma, P., Li, G., Meng, Q., Wu, T., 2014. Preformulation studies of myricetin: a
1060 natural antioxidant flavonoid. *Pharmazie* 69, 19–26.

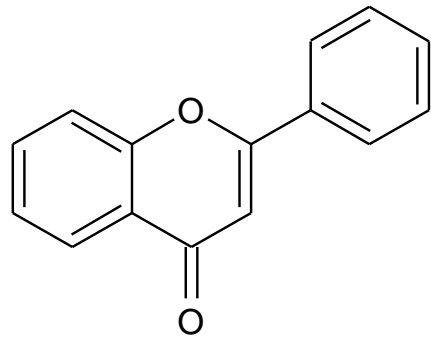
1061 Yu, Z., Guo, J., Hu, M., Gao, Y., Huang, L., 2020. Icaritin Exacerbates Mitophagy and Synergizes with
1062 Doxorubicin to Induce Immunogenic Cell Death in Hepatocellular Carcinoma. *ACS Nano* 14,
1063 4816–4828. <https://doi.org/10.1021/acsnano.0c00708>

1064 Zhou, Y., Wang, S., Ying, X., Wang, Y., Geng, P., Deng, A., Yu, Z., 2017. Doxorubicin-loaded redox-
1065 responsive micelles based on dextran and indomethacin for resistant breast cancer. *Int J*
1066 *Nanomedicine* 12, 6153–6168. <https://doi.org/10.2147/IJN.S141229>
1067 Zhu, B., Yu, L., Yue, Q., 2017. Co-delivery of vincristine and quercetin by nanocarriers for lymphoma
1068 combination chemotherapy. *Biomedicine & Pharmacotherapy* 91, 287–294.
1069 <https://doi.org/10.1016/j.biopha.2017.02.112>
1070

Figure 1. Chemical structure of flavonoid and their classes.

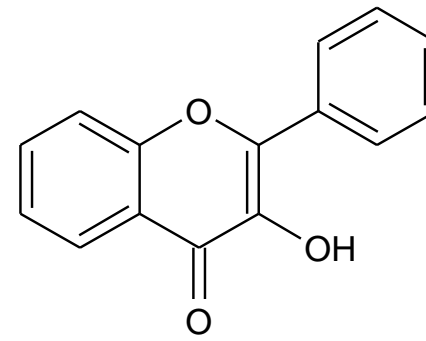
Figure 2. Total publications per year concerning flavonoids nanocarriers (web of science).

Figure 3. Total publications per year concerning flavonoids co-encapsulation (web of science).



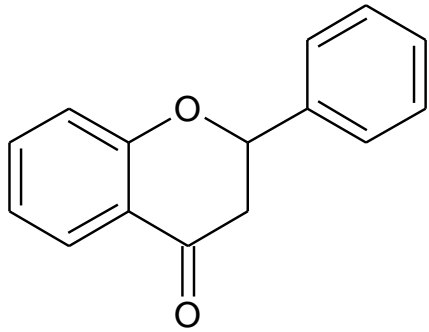
Flavone

e.g.: baicalein, baicalin (glucoside),
 icaritin (phenylated)



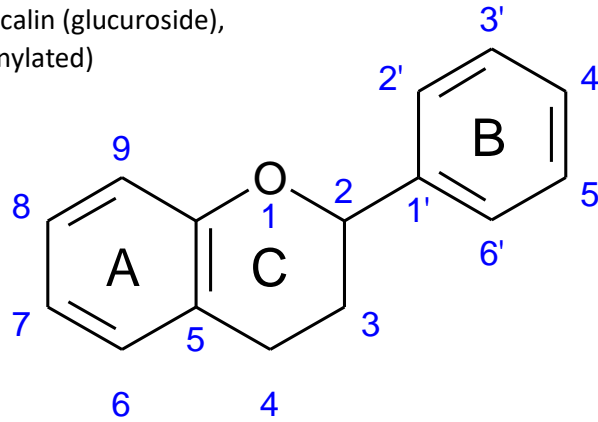
Flavonol

e.g.: quercetin

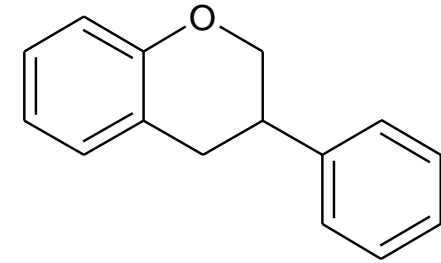


Flavanone

e.g.: naringenin, silibinin, silybin

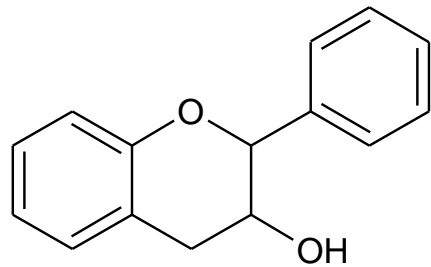


Flavonoid



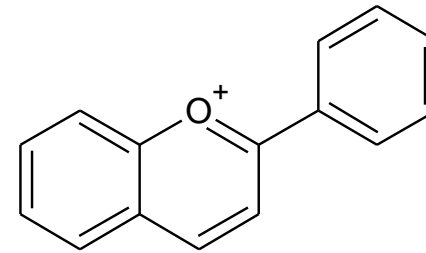
Isoflavonoid

e.g.: genistein (isoflavone)



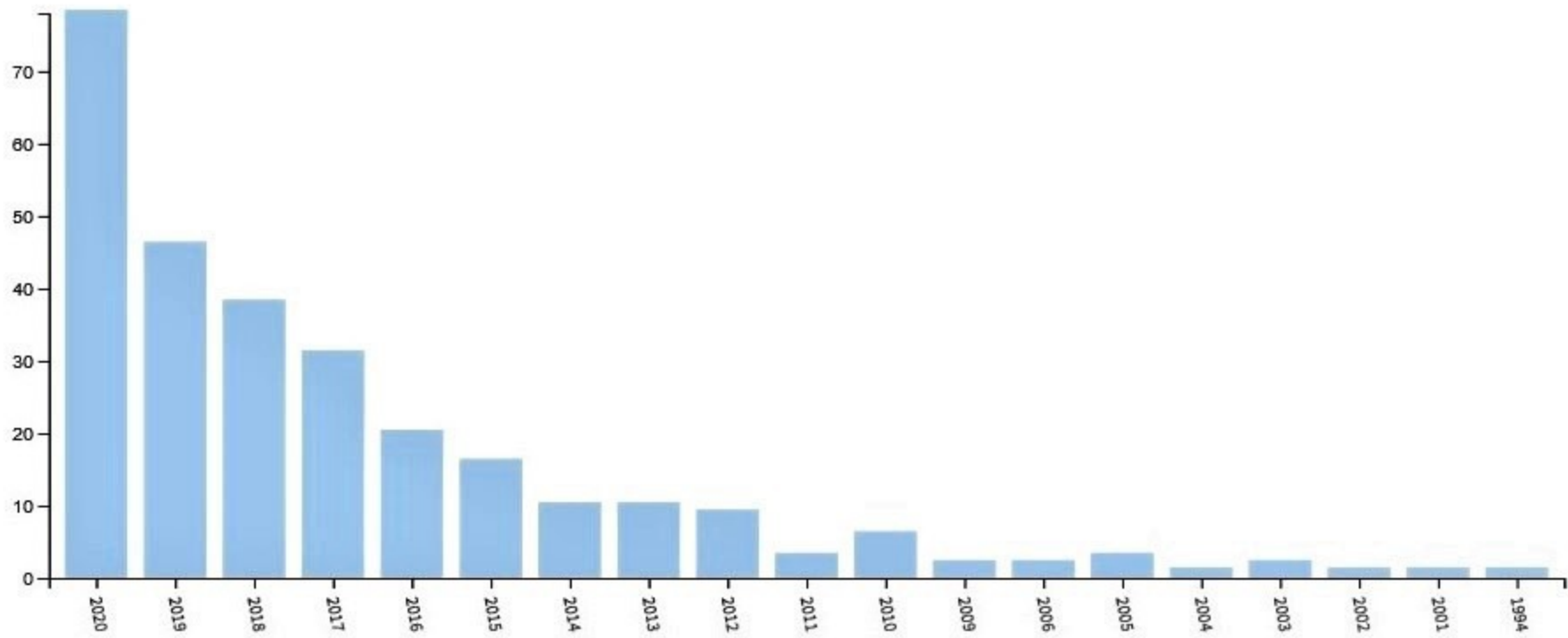
Flavanol

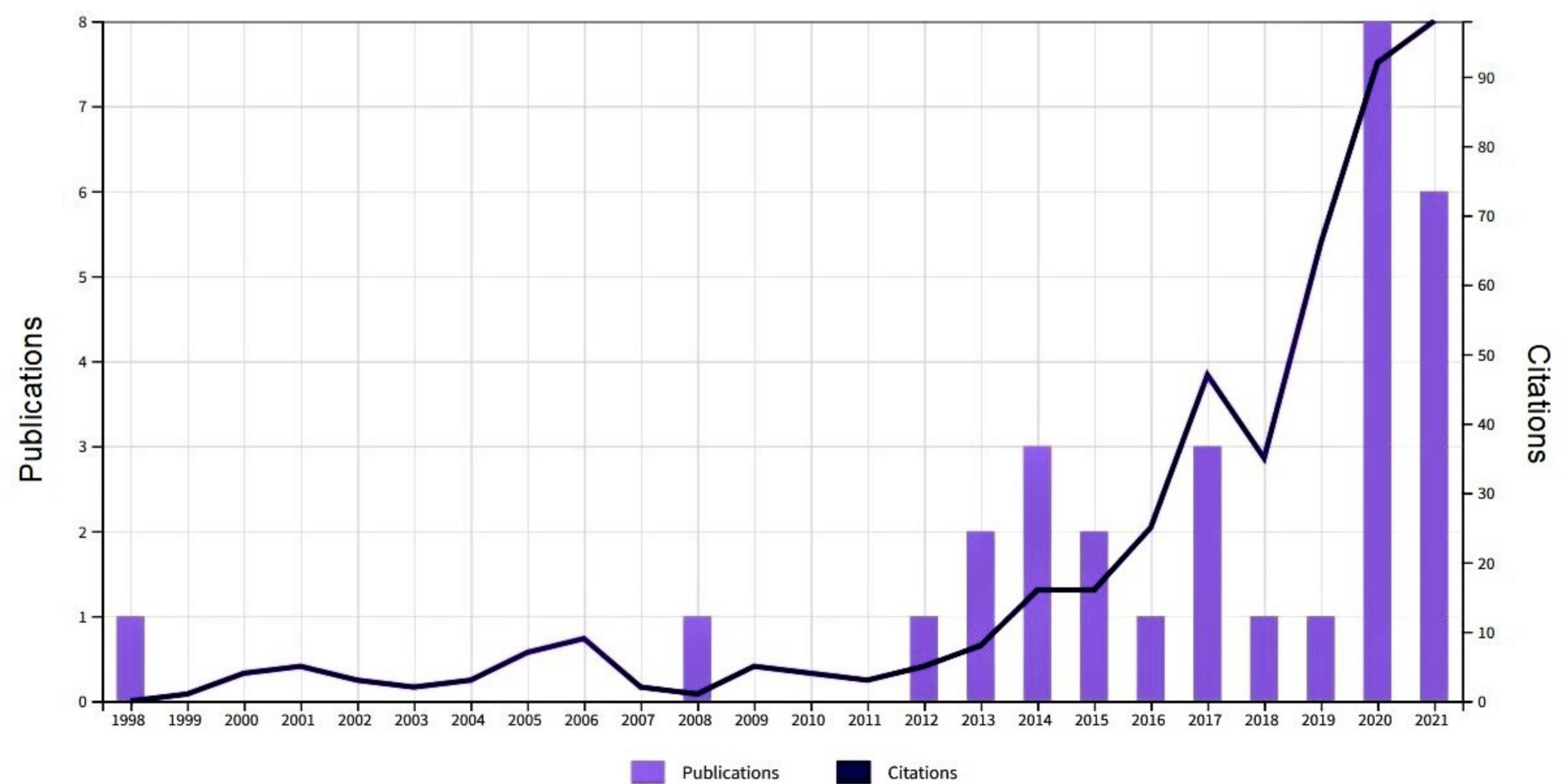
e.g.: epigallocatechin gallate

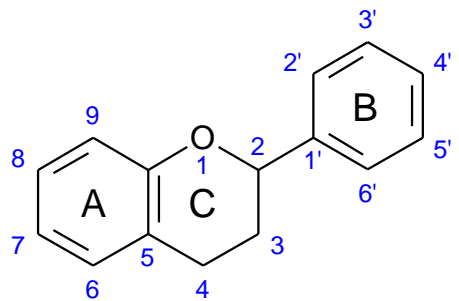


Anthocyanidin

Number of publications per year





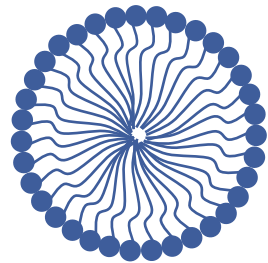


Flavonoid

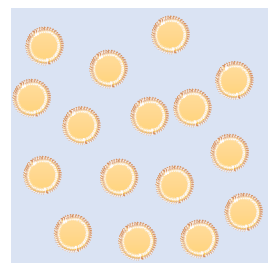


Anticancer drug

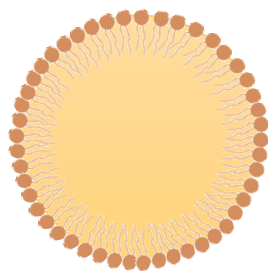
Co-encapsulation



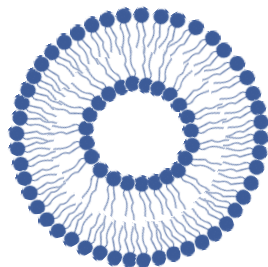
Micelle



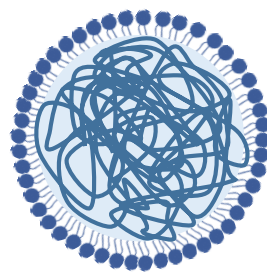
Nanoemulsion



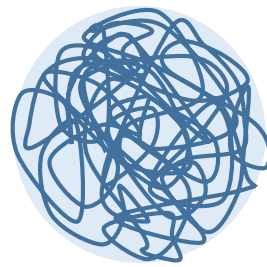
Solid Lipid Nanoparticle



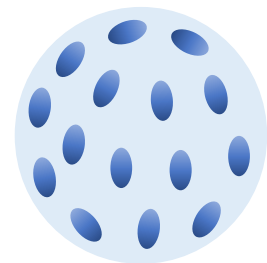
Liposome



Lipid-Polymer Hybrid Nanoparticle

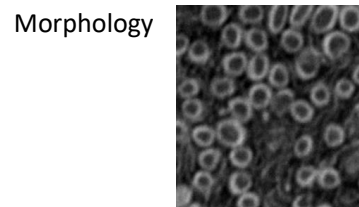
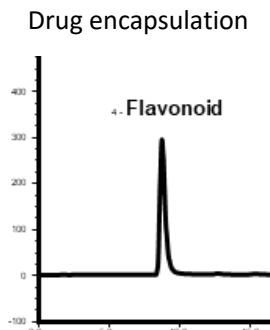
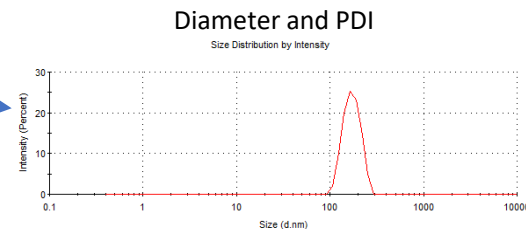


Polymeric Nanoparticle

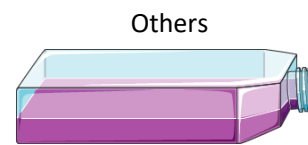
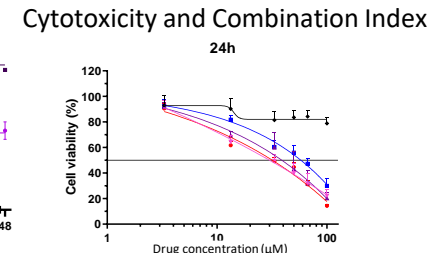
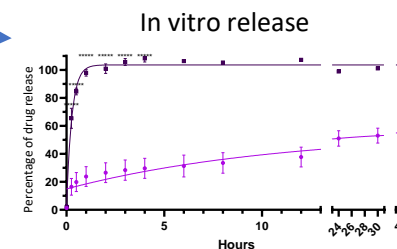


Mesoporous Silica Nanoparticle

Physico-chemical properties



In vitro prediction of the in vivo behavior



In vivo efficacy or mechanism assays

